

Design and Analysis of a Spar Beam for Vertical Tail of a Transport Aircraft.

A MAJOR PROJECT REPORT
SUBMITTED IN PARTIAL FULFILLMENT OF THE REQUIREMENTS FOR THE
AWARD OF
THE DEGREE OF

BACHELOR OF TECHNOLOGY

(Aerospace Engineering)

SUBMITTED TO
UNIVERSITY OF PETROLEUM AND ENERGY STUDIES, DEHRADUN

BY

Name of Students	University Roll No.
Condra Krishnakant	R290211008
Noman Zia	R290211014
Sanjay Thapa	R290211020

SUPERVISED BY
MR. VIJAY KUMAR PATIDAR
Assistant Professor

April 2015



COLLEGE OF ENGINEERING STUDIES
UNIVERSITY OF PETROLEUM AND ENERGY STUDIES, DEHRADUN

CERTIFICATE

We hereby certify that the work which is being presented in the project report entitled “Design and Analysis of A Spar Beam for Vertical Tail of a Transport Aircraft.” is in partial fulfilment of the requirements for the satisfactory performance for B. Tech. Aerospace Engineering. Minor Project submitted in the Department of Aerospace Engineering, University of Petroleum and Energy Studies, Dehradun is an authentic record of our own work carried out during a period from August 2014 to April 2015.

Submitted By:

Condra Krishnakant (R29021102008)

Noman Zia (R290211014)

Sanjay Thapa (R290211020)



This is to certify that the above statement made by the candidates is correct to the best of my knowledge.

Mr. Vijay Kumar Patidar
Assistant Professor
(Department Of Aerospace
Engineering)

Date: 13 April 2014

Dr. Om Prakash

Head of Aerospace Department

ACKNOWLEDGEMENT

It is a pleasure to thank all those great many people who helped, supported and encouraged us during this project work.

Firstly we express our sincere gratitude to Mentor, the guide of the project who carefully and patiently leant his valuable time and effort to give directions as well as to correct various documents with attention and care. .

We do also like to appreciate the consideration of the Project Coordinator, our Faculties and colleagues, which enabled us to balance our work along with this project. It was their attitude that inspired us to do such an efficient and apposite work.

We are indebted to those people across the globe who have shared their knowledge and perspectives in the form of online tutorials, forums and other resources which helped us to a great extend whenever we met with technical obstacles during this endeavour.

We wish to avail this opportunity to express a sense of gratitude and love to all our friends and our family for their unwavering support, strength, help and in short for everything they have done during the crucial times of the progress of our project.

Last but not the least we thank GOD ALMIGHTY for his blessings and guidance without which this dream project wouldn't have been reality

Condra Krishnakant

Noman Zia

Sanjay Thapa

ABSTRACT

Vertical & Horizontal Stabilizers are important structural components of an aircraft. Movement of the rudder controls the yawing of an aircraft whereas movement of elevator controls the pitching of an aircraft. The airloads on tail surfaces of general aviation airplanes are fairly low and single main spar with light stiffened skins are generally the typical construction of the horizontal stabilizer box, vertical stabilizer box, elevators and rudders. Structurally speaking vertical tail is a typical mini-wing construction. A major difference could be absence of ribs and multiple spars (more than 2) in the tail construction. Tails have symmetrical airfoil cross sections. Therefore in the absence of rudder or elevator deflection there is no aerodynamic load acting on the fuselage. However significant loads developed due to deflection and this is the major design load for the tail. For transport aircraft side gust load is also important from a design point of view. In this project a typical of a transport aircraft will be analysed. Loads representative of a small transport aircraft will be considered in this study. An efficient tapered spar beam will be designed for this load. SOM approach will be used for preliminary sizing of the spar.



LIST OF FIGURES

	Page No.
Fig. 1.1 Vertical Stabilizer structure arrangement	2
Fig. 1.2 Spar & Rib design	3
Fig. 1.3 Typical Spar Construction	4
Fig.1.4 Typical Rib Construction	4
Fig. 4.1 I-section beam	9
Fig. 4.2 Dimensions of the I-section	11
Fig.4.3 Isometric view of Uniform I-section beam	12
Fig. 4.4 Side view of Uniform I-section beam	13
Fig. 4.5 Isometric view of Tapered I-section beam	13
Fig. 4.6 Side view of Tapered I-section beam	14
Fig. 4.7 Mesh Uniform I-section beam having fixed end at left side with applied loads	15
Fig. 4.8 Mesh Tapered I-section beam having fixed end at left side with applied loads	16
Fig. 4.9 Displacement results for Uniform I-Section spar beam	17
Fig. 4.10 Stress results for Uniform I-Section spar beam	17
Fig. 4.11 Stress results for Tapered I-Section spar beam	18
Fig. 4.12 Displacement results for Tapered I-Section spar beam	18
Fig. 5.1 Isometric View of Tapered I-section beam with $t=8.205\text{mm}$	20
Fig. 5.2 Stress Distribution Contour of Tapered spar beam with $t=8.205\text{mm}$	20
Fig. 5.3 Maximum Stress Region	21
Fig. 5.4 Detailed View	21
Fig. 5.5 Displacement results for Tapered spar beam with $t=8.205\text{mm}$	22
Fig. 5.6 Stress Distribution Contour of Tapered spar beam with $t=6.2\text{mm}$	22
Fig. 5.7 Maximum Stress Region	23
Fig. 5.8 Displacement results for Tapered spar beam with $t=6.2\text{mm}$	23

Fig. 5.9 Stress Distribution Contour of Tapered spar beam with $t=3.5\text{mm}$	24
Fig. 5.10 Maximum Stress Region	24
Fig. 5.11 Detailed View	25
Fig. 5.12 Displacement results for Tapered spar beam with $t=3.5\text{mm}$	25
Fig. 5.13 Cutout Model	26
Fig. 5.14 Isometric View of Tapered spar beam with cutouts	27
Fig. 5.15 Side view of Tapered spar beam with cutouts	28
Fig. 5.16 Close view of Tapered spar beam with cutouts	28
Fig. 5.17 Mesh model of Tapered spar beam with cutouts	28
Fig. 5.18 Stress Distribution Contour of Tapered spar beam with vertical cutouts for $t=6.2\text{mm}$	29
Fig. 5.19 Maximum Stress Region	29
Fig. 5.20 Detailed View	30
Fig. 5.21 Displacement results for Tapered spar beam with vertical cutouts for $t=6.2\text{mm}$	30
Fig. 5.22 Stress Distribution Contour of Tapered spar beam with vertical cutouts for $t=3.5\text{mm}$	31
Fig. 5.23 Maximum Stress Region	31
Fig. 5.24 Detailed View	32
Fig. 5.25 Displacement results for Tapered spar beam with vertical cutouts for $t=3.5\text{mm}$	32
Fig. 5.26 Cutout Model	33
Fig. 5.27 Stress Distribution Contour of Tapered spar beam with horizontal cutouts for $t=6.2\text{mm}$	34
Fig. 5.28 Maximum Stress Region	34
Fig. 5.29 Detailed View	35
Fig. 5.30 Displacement results for Tapered spar beam with horizontal cutouts for $t=3.5\text{mm}$	35
Fig. 5.31 Stress Distribution Contour of Tapered spar beam with horizontal cutouts for $t=6.2\text{mm}$	35
Fig. 5.32 Maximum Stress Region	36

Fig. 5.33 Detailed View	36
Fig. 5.34 Displacement results for Tapered spar beam with horizontal cutouts for $t=3.5\text{mm}$	37
Fig. 5.35 Side View of Tapered spar beam with mixed cutouts	37
Fig. 5.36 Isometric View of Tapered spar beam with mixed cutouts	38
Fig. 5.37 Stress Distribution Contour of Tapered spar beam with 10 horizontal cutouts & 6 vertical cutouts	40
Fig. 5.38 Maximum Stress Region	40
Fig. 5.39 Detailed View	41
Fig. 5.40 Displacement results for Tapered spar beam with 10 horizontal cutouts & 6 vertical cutouts	41
Fig. 5.41 Stress Distribution Contour of Tapered spar beam with 10 horizontal cutouts & 3 vertical cutouts	43
Fig. 5.42 Maximum Stress Region	43
Fig. 5.43 Detailed View	44
Fig. 5.44 Displacement results for Tapered spar beam with 10 horizontal cutouts & 3 vertical cutouts	44
Fig. 5.45 Stress Distribution Contour of Tapered spar beam with 9 horizontal cutouts & 3 vertical cutouts	45
Fig. 5.46 Maximum Stress Region	46
Fig. 5.47 Detailed View	46
Fig. 5.48 Displacement results for Tapered spar beam with 9 horizontal cutouts & 3 vertical cutouts	47
Fig. 6.1 Moment of Inertia at different station	48
Fig. 6.2 Stress at different stations	50
Fig. 7.1 Thickness iteration result plot	52
Fig. 7.2 Cutout iteration result plot	53
Fig. 7.3 Mixed Cutout iteration result plot	54

LIST OF TABLE

	Page No.
Table 4.1 Stress & Deflection Calculations of different cross-sections	9
Table 4.2 Dimensions of I-sections at different Stations	11
Table 4.3 Meshing Parameters	13
Table 5.1 Dimensions of Vertical Cutouts	24
Table 5.2 Dimensions of Horizontal Cutouts	30
Table 5.3 Dimensions of Horizontal Cutouts	34
Table 5.4 Dimensions of Vertical Cutouts	35
Table 5.5 Dimensions of Horizontal Cutouts	37
Table 5.6 Dimensions of Vertical Cutouts	37
Table 5.7 Dimensions of Horizontal Cutouts	40
Table 5.8 Dimensions of Vertical Cutouts	40
Table 6.1 Moment of Inertia calculation at different station	43
Table 6.2 Bending stress calculation at different station for Uniform I-section beam	43
Table 6.3 Bending stress calculation at different station for Tapered I-section beam	44
Table 7.1 UTS of beams	47
Table 7.2 Experimental value of Aluminium 2024 T-3	47
Table 7.3 Thickness Iteration result	48
Table 7.4 Cutout Iteration results	48
Table 7.5 Mixed Cutout Iteration results	49

TABLE OF CONTENTS

	Page No.
<i>Acknowledgement</i>	<i>i</i>
<i>Abstract</i>	<i>ii</i>
<i>List of Figures</i>	<i>iii-v</i>
<i>List of Tables</i>	<i>vi</i>
1. Introduction	1-5
1.1 Design Motivation	1
1.2 Introduction	1-2
1.3 Vertical Stabilizer	2-3
1.4 General Layout	3-4
1.5 State of the Art	5
1.6 Motivation & Scope of the present work	5
2. Literature Survey	6
3. Aim & Objectives	7
3.1 Aim	7
3.2 Objectives	7
4. Methodology	8-18
4.1 Selection of Cross-section of spar beam	8-10
4.2 Modelling	10-15
4.2.1 Uniform I-section beam cross-sectional area	11
4.2.2 Tapered I-section beam cross-sectional area	11-15

4.3 Meshing	16
4.4 Analysis	16-18
5. Optimization of Spar Beam	19-43
5.1 Definition of Optimization problem	19
5.2 Design variable for the optimization problem	19-2
5.2.1 Thickness Iteration	19-25
5.2.2 Cutouts Iteration	25-46
6. Calculations	47-49
6.1 Calculation of Moment of Inertia at different stations	47
6.2 Bending stress for Uniform I-section cross-sectional area	48
6.3 Bending stress for Tapered I-section cross-sectional area	48-49
7. Results & Conclusions	50-53
8. References	54

1. INTRODUCTION

1.1 Design Motivation

1.2 Introduction

Structural and Multi-disciplinary Optimizations have been gaining more attention in recent years for their contributions in the design enhancement, especially in the early stages of product development. When a modern full-loaded subsonic aircraft takes off, only 20% of its total weight is payload. Of the remaining 80%, roughly half is aircraft empty weight and the other half is fuel weight. Hence, any saving in structural weight can lead to a corresponding increase in payload. Alternatively, for a given payload, saving in aircraft weight means reduced fuel requirements. Therefore, it is not surprising that the aircraft manufacturers are prepared to invest heavily in weight reduction.

1.3 Vertical Stabilizer

The root of the box is terminated at the aft fuselage juncture with fittings or splices or the box spars terminate on bulkheads in the aft fuselage that are canted (for swept fin) into the plane of the spars as shown in figure, thus transmitting the fin loads directly into the fuselage structure and avoiding the fatigue-critical structural splices.

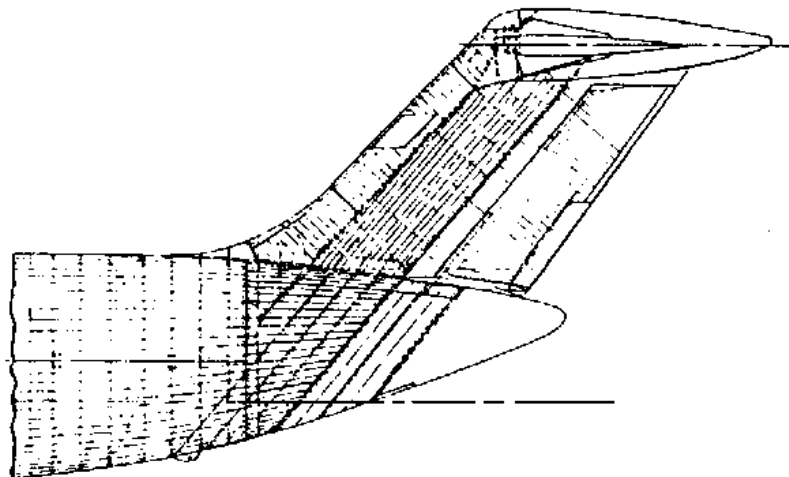


Fig. 1.1 Vertical stabilizer structure arrangement

The T-tail arrangement places the horizontal stabilizer in a favourable flow field during low-speed, high angle-of-attack operations. Mounting the horizontal stabilizer on top of the fin has significant effect on the torsional frequency of the fin.

The span of the T-tail fin is approximately one-third shorter than conventional tails, but, on the other hand, the higher structural stiffness is required. Therefore, typical skin-stringers or integrally stiffened panels are suitable for this requirement.

Loads on vertical tail are caused by the following:

- Rudder deflection
- Aileron deflection
- Lateral gust
- Asymmetric engine thrust

1.4 General Layout of Vertical Stabilizer Structure

A real commercial aircraft vertical stabilizer contains a large number of structural components. Creation of a detailed vertical tail model by simultaneously incorporating all the features is virtually impossible. Thus, engineers rely on simplified models that provide a fairly accurate approximation of the real wing structural behaviour. Moreover, it is rare to find a design procedure that starts off with a detailed approach. Most commonly, the design is a multi-step process where the initial steps contemplate simplified configurations and each step inherits properties from the previous ones. Therefore, the importance of obtaining initial designs is to guarantee that its best features will pass on to subsequent steps.

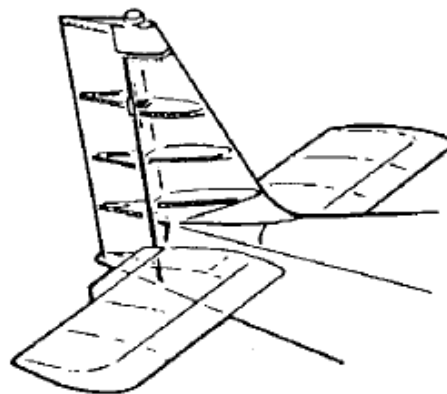


Fig. 1.2 Spar & Rib Design

The vertical stabilizer picks up the air loads and transmits them to the fuselage through spars.

Vertical stabilizer consists of basic structural elements like, the front and rear spars, ribs positioned at different stations along the span-wise direction, the stringers running along the span and skins covering these internal components. Each of these component act like a beam and a torsion member as a whole.

A typical spar construction is depicted in Figure.

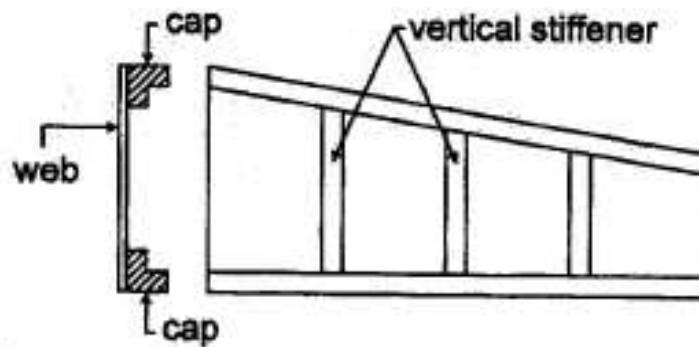


Fig. 1.3 Typical spar construction

Ribs are planar structures capable of carrying in-plane loads and are placed along the span of the stabilizer.

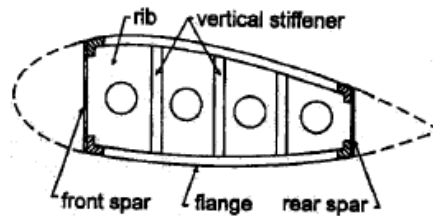


Fig. 1.4 Typical rib construction

1.5 State of the Art

The complexity of the structural configuration of an aircraft combined with a wide range of loading and boundary conditions requires a multilevel optimization approach. Because of its size and complexity, there is a clear need for advanced tools integrating and accelerating the design process.

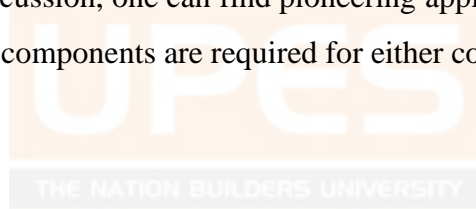
The economic performance of an aircraft depends very much on its overall weight. It is important to minimize structural weight, in order to reduce fuel consumption and operating

costs every time the aircraft flies. Modern aircraft design therefore utilizes high performance materials with high strength to weight ratios. This when combined with efficient analysis and optimization tools, can lead to a significant increase in the strength and reliability, while reducing the structural weight of the components. Optimization of aerospace structures, such as vertical tail, however represents a very complex task with literally hundreds of design variables. It is therefore not surprising that, despite the dramatic increase in computational power over the past twenty years, optimization is still best carried out as a multilevel process.

1.6 Motivation and Scope of the Present Work

This project consists of development of design optimization environment. The loads coming from different flight conditions vary from root to tip of the vertical stabilizer. These loads are used to size different components of an aircraft vertical stabilizer, like spar web, web caps (flanges) etc. The main objective of the present work is to develop efficient and accurate design optimization methodologies to design the complete spar.

From the previous discussion, one can find pioneering applications in aerospace industry where lightweight structural components are required for either cost reductions or to increase payload.



2. LITERATURE SURVEY

2.1 Design and Analysis of A Spar Beam For The Vertical Tail of A Transport Aircraft. Vinod S. Muchchandi, S. C. Pilli. Department of Mechanical.

- Finite Element Analysis
- Spar Beam Optimization
- Loads and boundary conditions

2.2 Immanuel D, Arulselvan K, Maniiarasan P, Senthilkumar S (2014) 'Stress Analysis and Weight Optimization of a Wing Box Structure Subjected To Flight Loads', The International Journal Of Engineering And Science (IJES), 3(1), pp. 33-40

- Selection of spar beam
- Theoretical calculations of Spar Beam

2.3 Sridhar Chintapalli (2006) Preliminary Structural Design Optimization of an Aircraft Wing-Box, Concordia University, Montreal, Canada.

- Wing loads and theoretical calculations.
 - Finite element analysis of wing.
-

3. AIM & OBJECTIVES

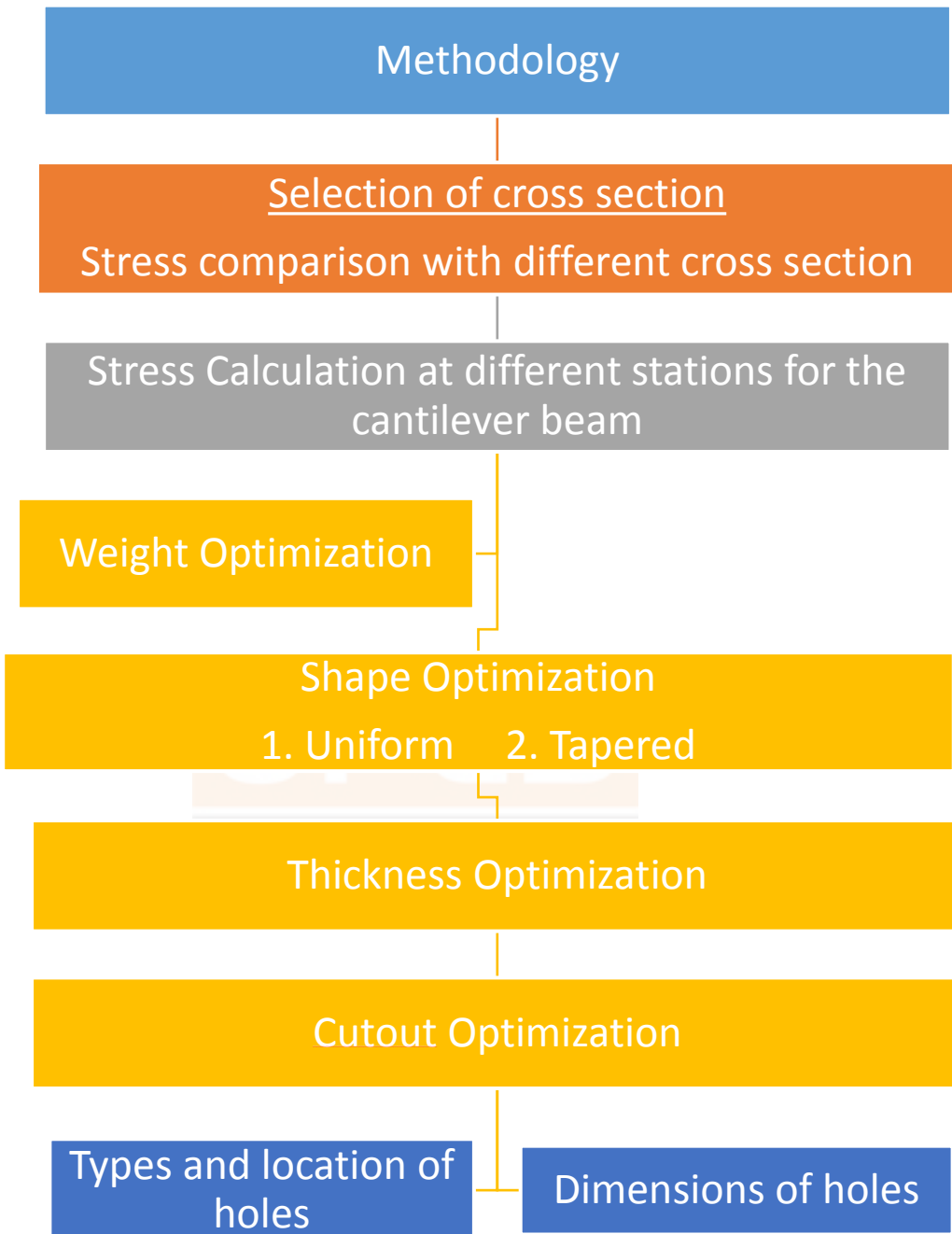
3.1 Aim

Design and analysis of a Spar Beam for Vertical Tail of a Transport Aircraft.

3.2 Objectives

- A typical transport aircraft wing spar design will be considered and the initial design will be carried out using conventional design approach.
 - A finite element approach will be used to calculate the stresses developed at each station for a given bending moment.
 - Several iterations will be carried out for design optimization of the spar beam.
 - A typical material will be chosen as the material for spar beam and linear static analysis will be used for the stress analysis.
 - Spar beam will be designed to yield at the design limit load and material saving will be achieved through the design optimization.
-
-

4. METHODOLOGY



4.1 Selection of cross-section of spar beam

I-shaped cross-sections are very common choices for aircraft spars.

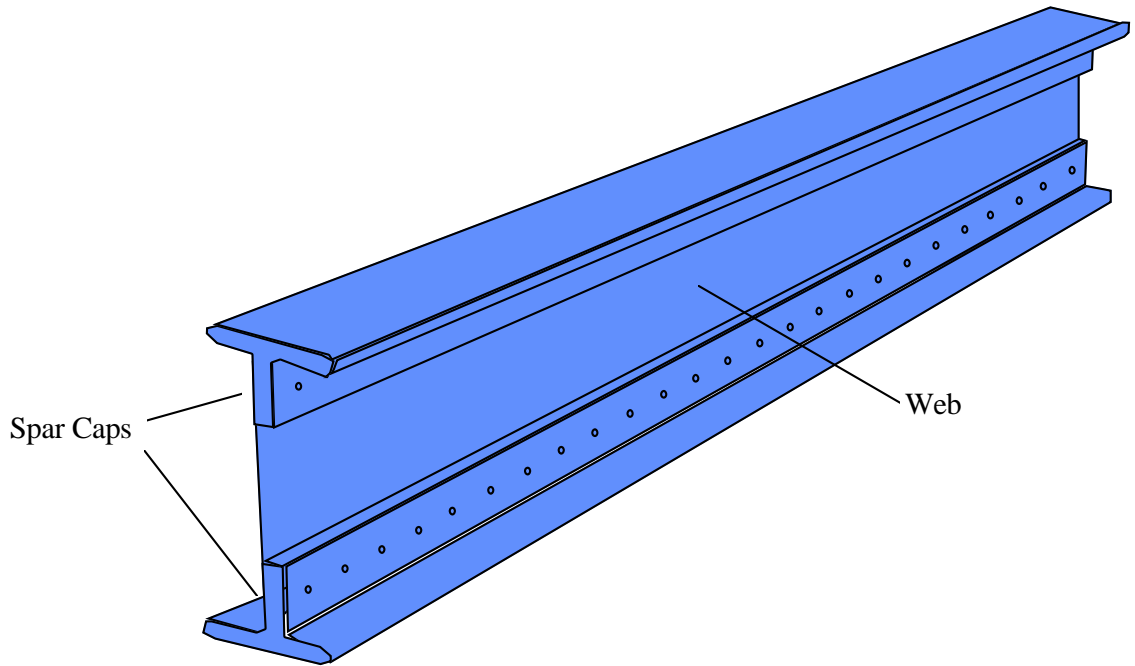


Fig. 4.1 I-section beam.

- **Bending Stresses, $\sigma = My/I$**

where, **I = Moment of Inertia,**

M = Bending Moment &

y = Distance of the top surface from neutral axis

Also, $\sigma = \frac{M}{(I/y)}$

Section Modulus, $Z = I / y$

I cross-section beam is the best spar beam because its section modulus is high due to its high moment of inertia ($Z \propto I$). Therefore, Stresses induced in the beam will be lower.

Table 4.1 Stress & Deflection Calculations for different cross-sections

Cross Section	Stress(kg/mm ²)	Deflection(mm)
---------------	-----------------------------	----------------

Circle	39.243	26.3
Circle with hole	12.65	4.64
Square	33.212	25
Rectangle	23.48	12.5
I-section	7.899	2.5239

4.2 Modelling

Modelling of the design of the spar beam having I-section cross-sectional area is done in CATIA V5 R18. There are two types of model i.e.

1. Uniform I-section cross-sectional area.
2. Tapered I-section cross-sectional area.

The Relation for dimensions for a given D is:

$$B=0.5D,$$

$$t=0.05D,$$

$$b=0.45D,$$

$$d=0.9D$$

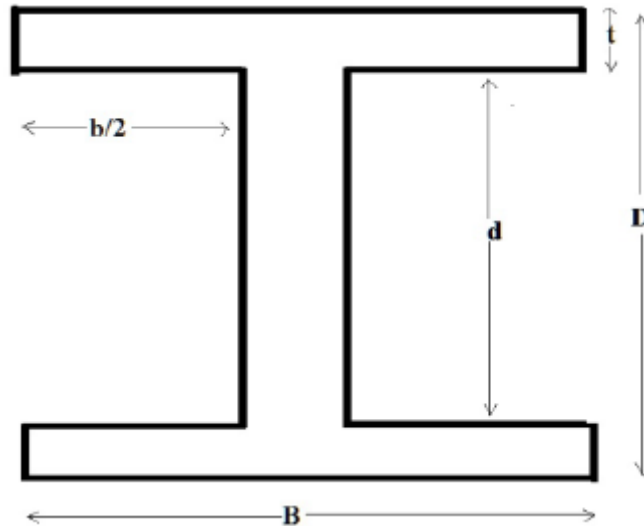


Fig. 4.2 Dimensions of the I-section

4.2.1 Uniform I-section cross-sectional area:

The Dimensions of the Uniform I section beam are:

$$D = 164.106\text{mm}$$

$$B = 82.053 \text{ mm}$$

$$d = 147.695 \text{ mm}$$

$$b = 73.847 \text{ mm}$$

$$t = 8.2053 \text{ mm}$$

$$\text{Length of the beam} = 3250 \text{ mm}$$

There are 10 stations defined at 325 mm distance apart.

4.2.2 Tapered I-section Cross-sectional area:

The Dimensions of the Uniform I section beam are:

$$\text{Length of the beam} = 3250 \text{ mm}$$

There are 10 stations defined at 325 mm distance apart. The dimension at each station is:

Design and Analysis of A Spar Beam for Vertical Tail of a Transport Aircraft.

Table 4.2 Dimensions of I-section at different stations (in mm)

Station No.	D	B	t	d
0	164.106	82.053	8.2053	147.6954
1	149.1	74.55	7.455	134.19
2	134.084	67.042	6.7042	120.6756
3	119.054	59.527	5.9527	107.1486
4	104.003	52.0015	5.20015	93.6027
5	88.921	44.4605	4.44605	80.0289
6	73.789	36.8945	3.68945	66.4101
7	58.566	29.283	2.9283	52.7094
8	43.152	21.576	2.1576	38.8368
9	27.184	13.592	1.3592	24.4656
10	13.592	6.796	0.6796	12.2328

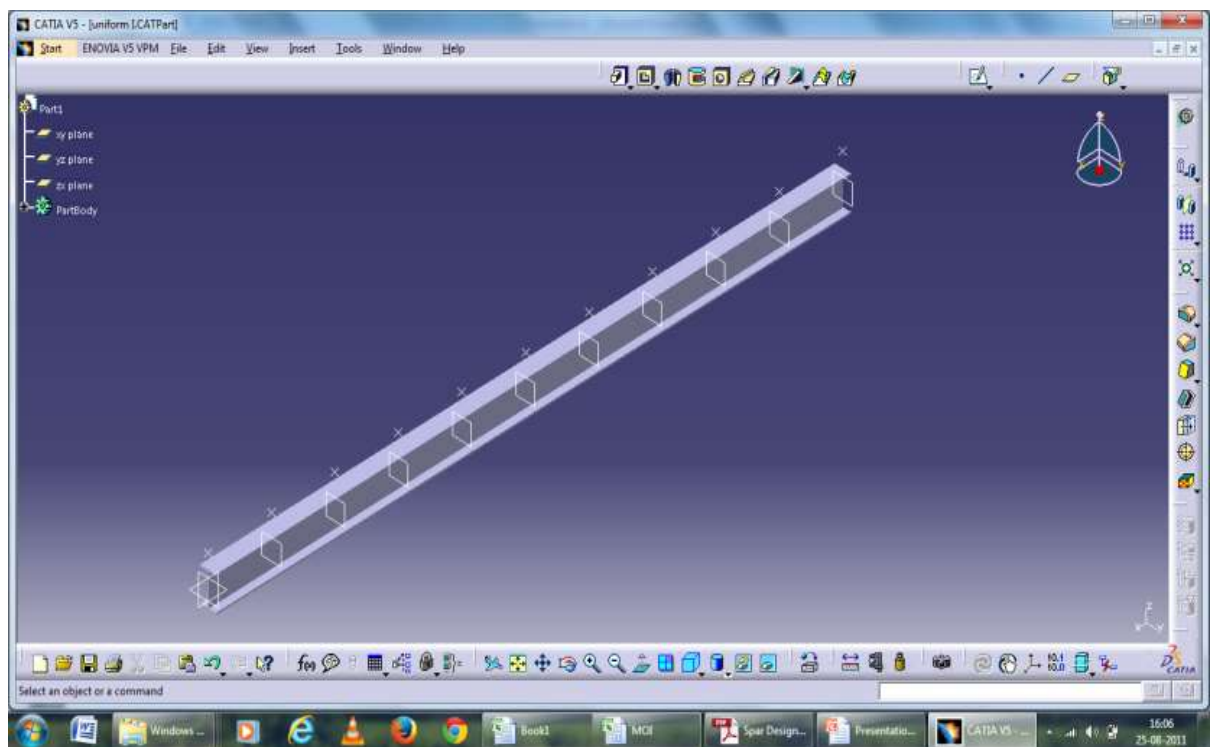


Fig. 4.3 Isometric View of Uniform I-section beam.

Design and Analysis of A Spar Beam for Vertical Tail of a Transport Aircraft.

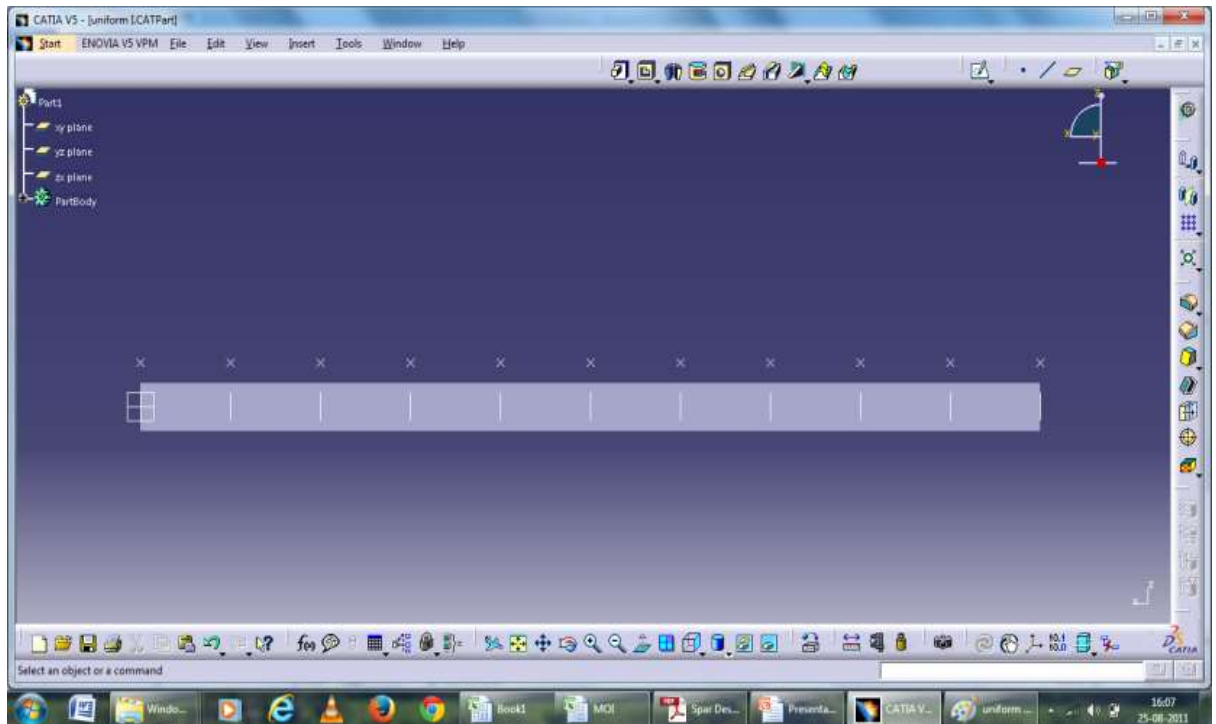


Fig. 4.4 Side View of Uniform I-section beam.

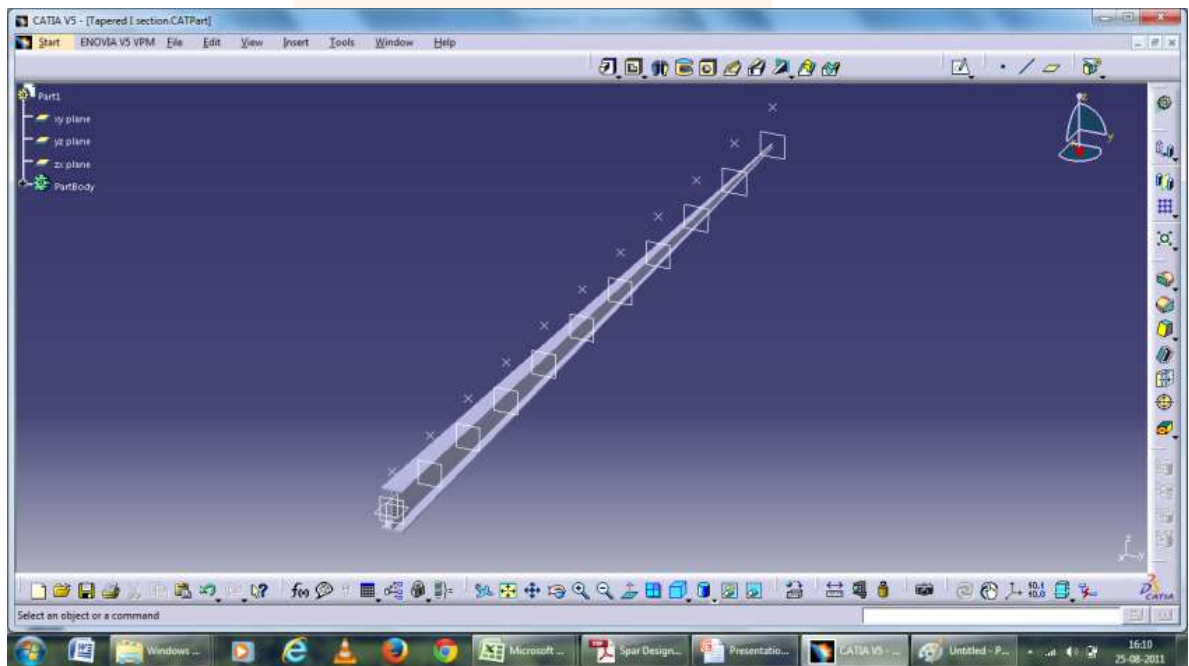


Fig. 4.5 Isometric View of Tapered I-section beam.

Design and Analysis of A Spar Beam for Vertical Tail of a Transport Aircraft.

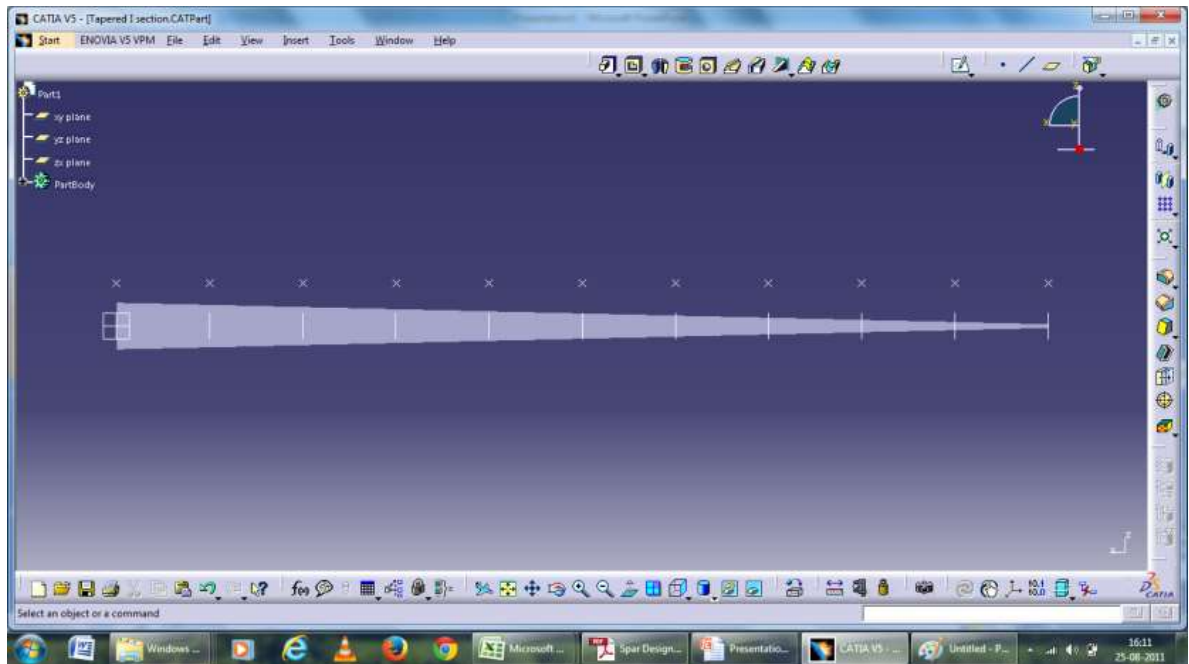
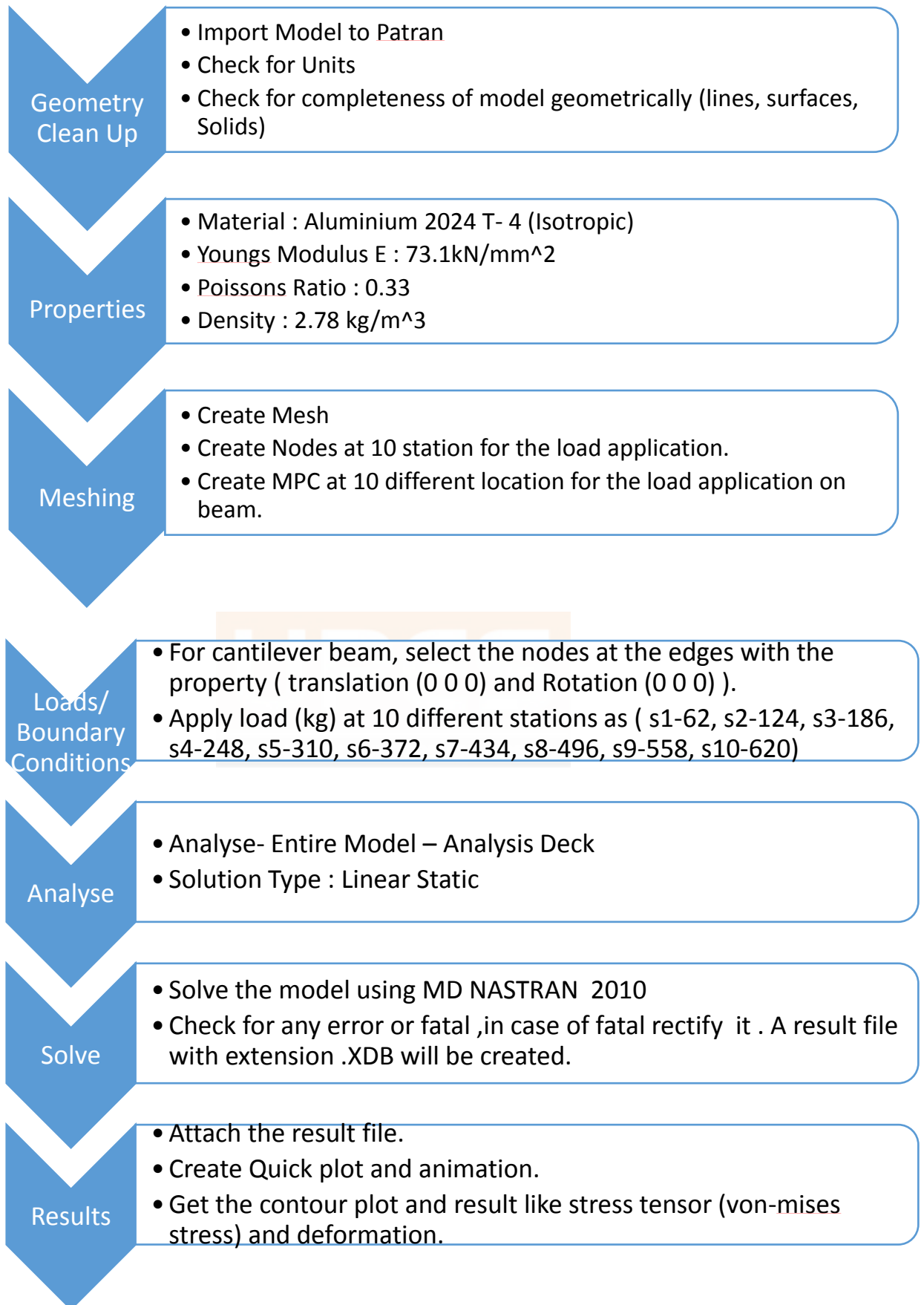


Fig. 4.6 Side View of Tapered I-section beam.





4.3 Meshing

Isotropic material property is applied.

Material used is Aluminium 2024-T3 with density is 2.780 g/cm^3 , modulus of elasticity 73.1 KN/mm^2 and Poisson's ratio is 0.33.

3-Dimensional solid meshing is performed.

Tert-10 elements are used for 3-D meshing.

Table 4.3 Meshing Parameters

Model	Nodes	Elements
Uniform I- section beam	10358	4887
Tapered I- section beam	13589	6464

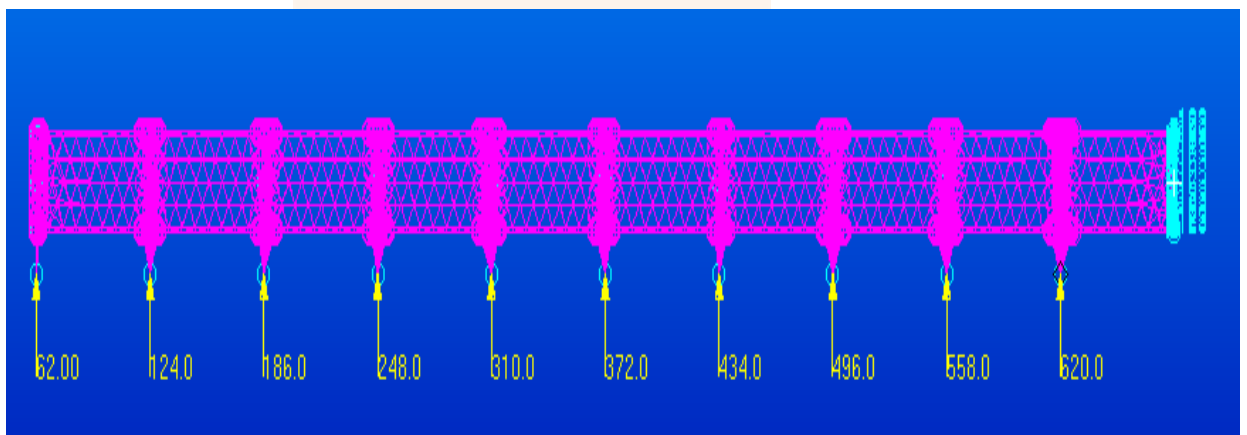


Fig. 4.7 Meshed Uniform I-section beam having fixed end at left side with applied loads.

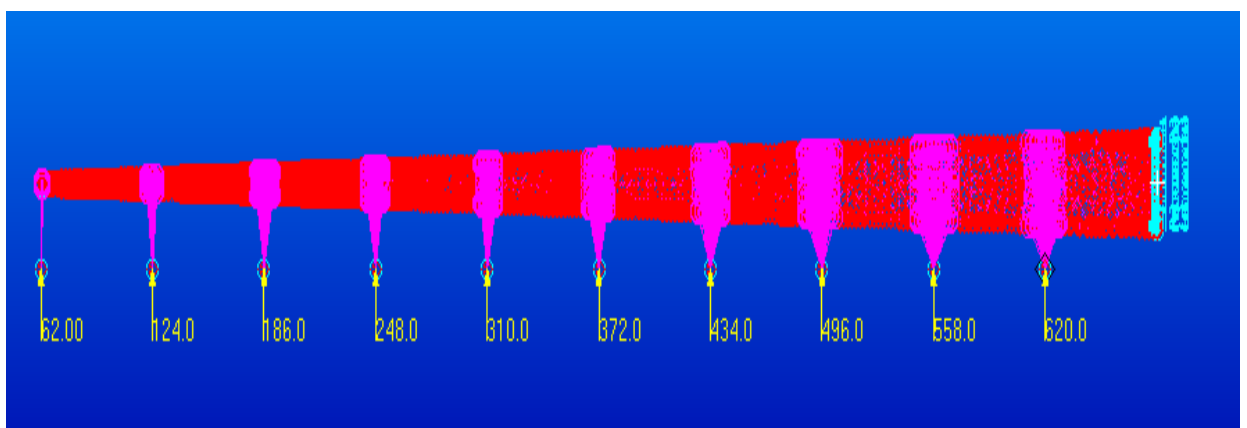


Fig. 4.8 Meshed Tapered I-section beam having fixed end at left side with applied loads.

4.4 Analysis

Different loads are applied at different stations as per the reference paper.

One end is kept fixed by the edge nodes element.

Contour graphs are plotted for deflection and for stress tensor.

Identify the area of the section and estimate approximately the stress and deflection.

Analyse the contour and identify the stress distribution.

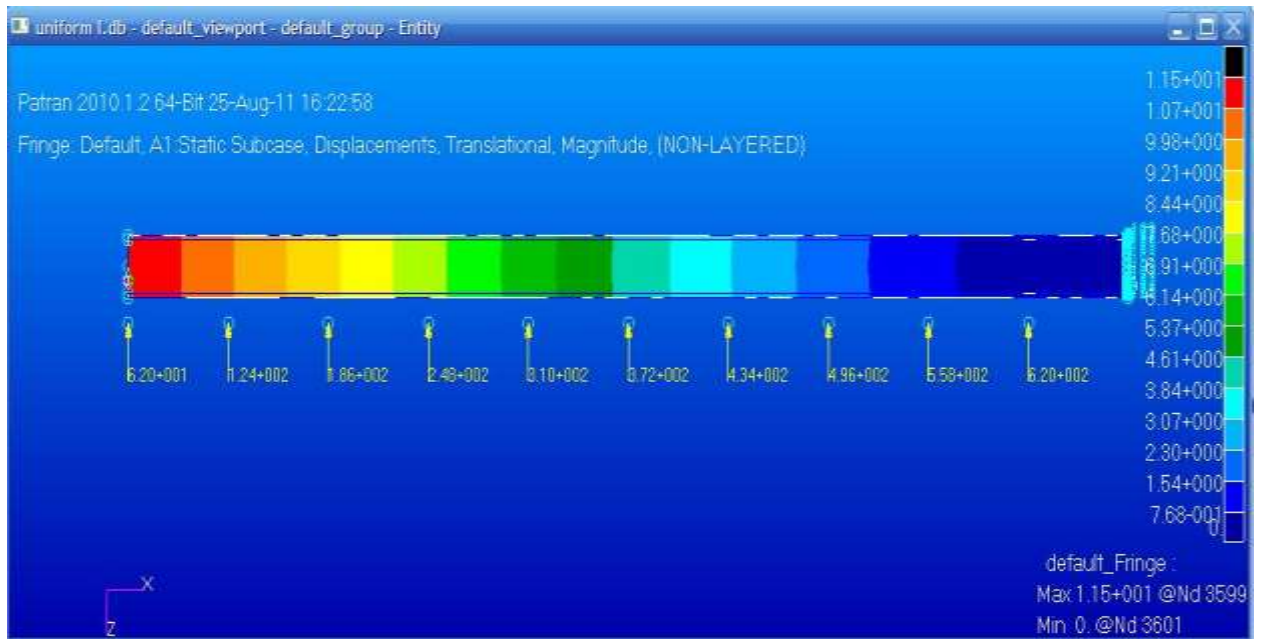


Fig. 4.9 Displacement results for Uniform I-section Spar beam.



Fig. 4.10 Stress results for Uniform I-section Spar beam.

Design and Analysis of A Spar Beam for Vertical Tail of a Transport Aircraft.

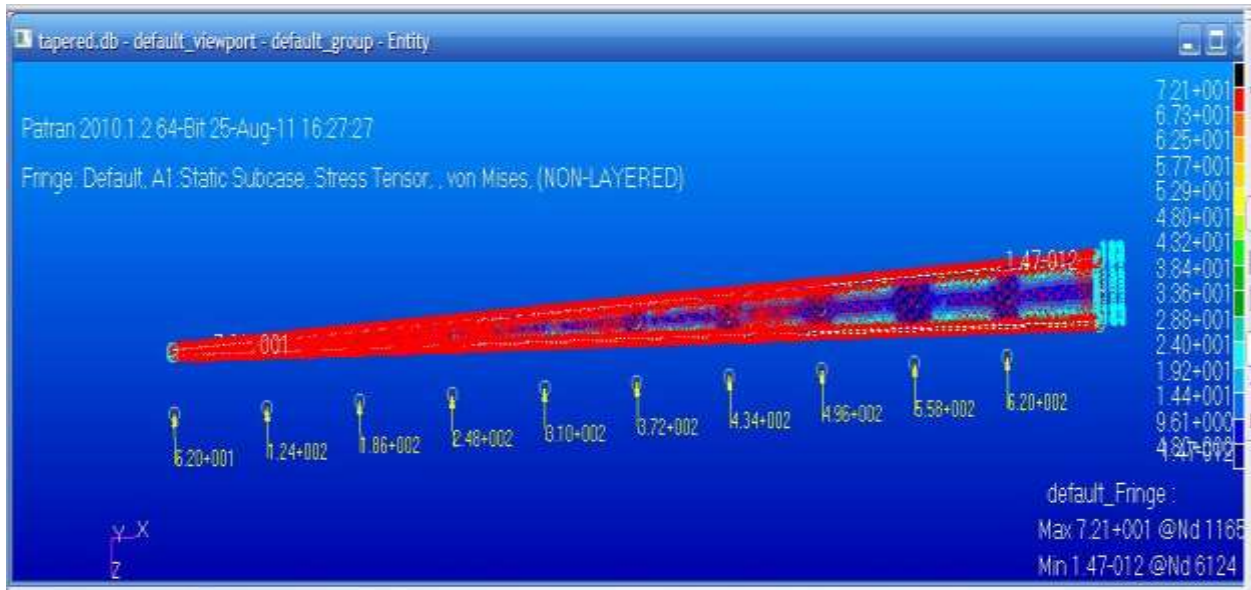


Fig. 4.11 Stress results for Tapered I-section Spar beam.

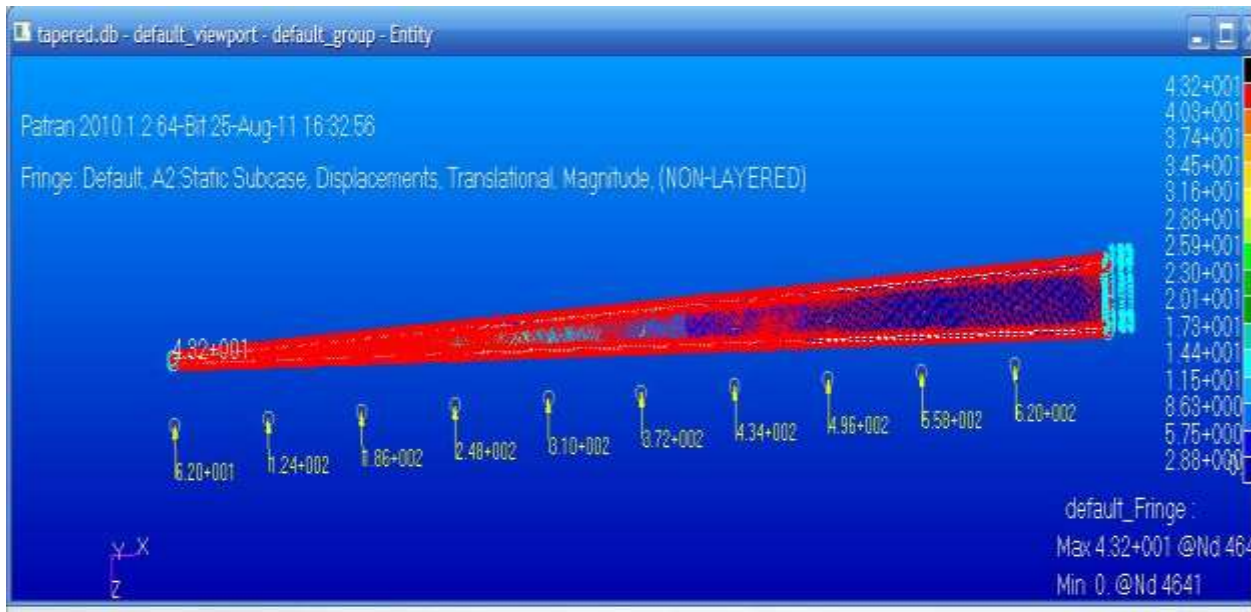


Fig. 4.12 Displacement results for Tapered I-section Spar beam.

5. OPTIMIZATION OF SPAR BEAM

5.1 Definition of the Optimization Problem

Any optimization problem is defined in terms of three essential components namely, the design variables, the constraints and the objective function. Design variables are independent quantities that are varied in order to achieve the optimum design. Upper and lower limits, usually called as side constraints are specified on design variables. The third essential component of an optimization problem, the objective or the weight function, is also a function of the design variables. The solution of an optimization problem is a set of allowed values for the design variables for which the objective function assumes an 'optimal value'. In mathematical terms, optimization usually involves maximizing or minimizing the objective function.

5.2 Design Variable for the Optimization Problem

The design variable for this problem is identified as 't' which is spar thickness. Using t, different dimensions of the spar beam can be obtained from design practice relations.

5.2.1 Thickness Iterations

- **Iteration 1: $t = 8.205\text{mm}$**

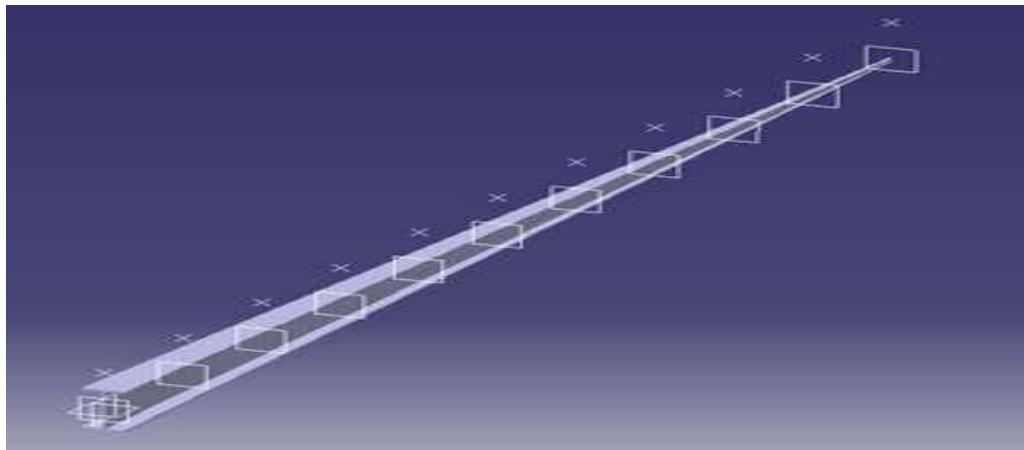


Fig. 5.1 Isometric View of Tapered I-section beam with $t = 8.205\text{mm}$

After applying the loads on the spar beam, it is solved using NASTRAN and the results are accessed in PATRAN.

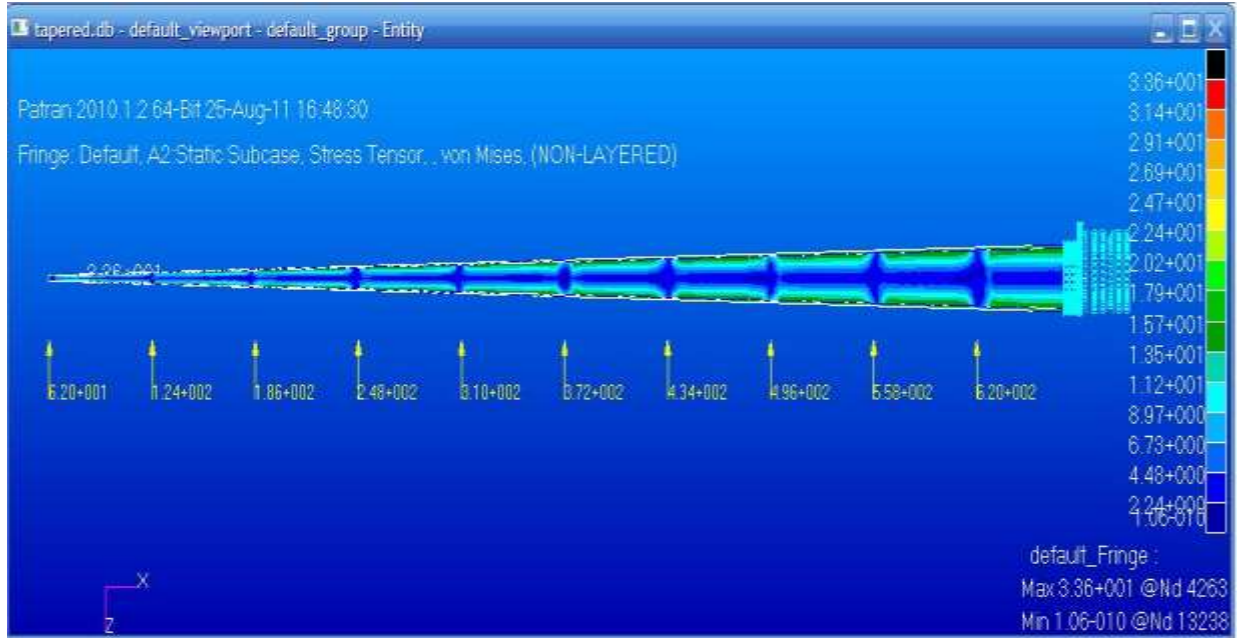


Fig. 5.2 Stress Distribution Contour of Tapered Spar Beam with $t = 8.205\text{mm}$

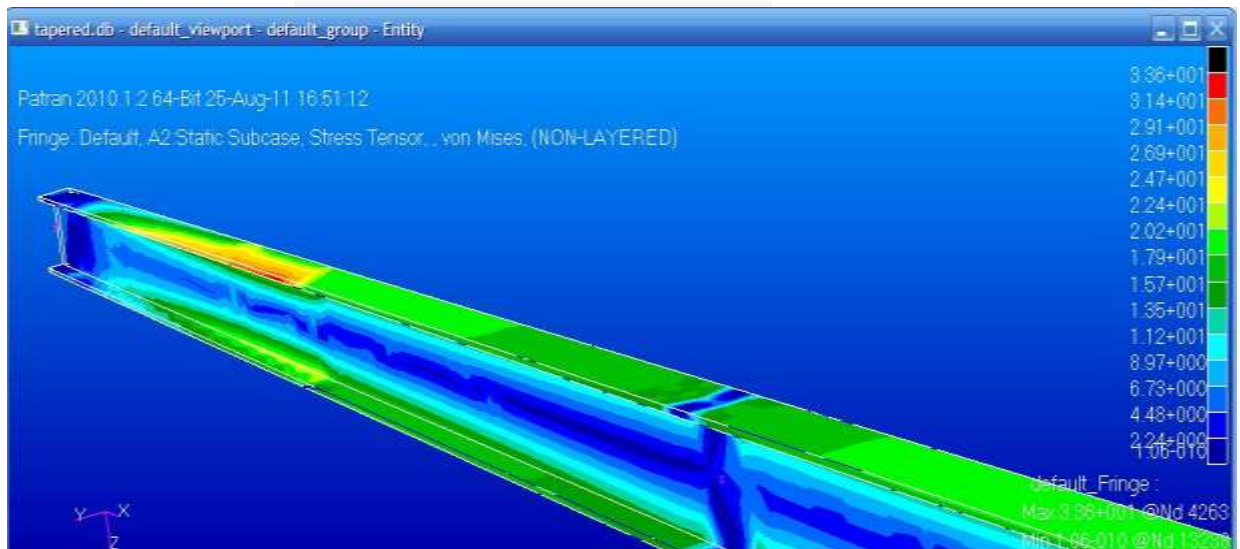


Fig. 5.3 Maximum Stress Region

After applying loads (as shown in Fig. 5.2) and boundary condition, maximum stress value is found to be 72.1 MPa which is much less than the yield strength of the material. Therefore, this case is valid for the design of spar beam.

Hence, the second iteration will be carried out for reduced thickness.

Design and Analysis of A Spar Beam for Vertical Tail of a Transport Aircraft.

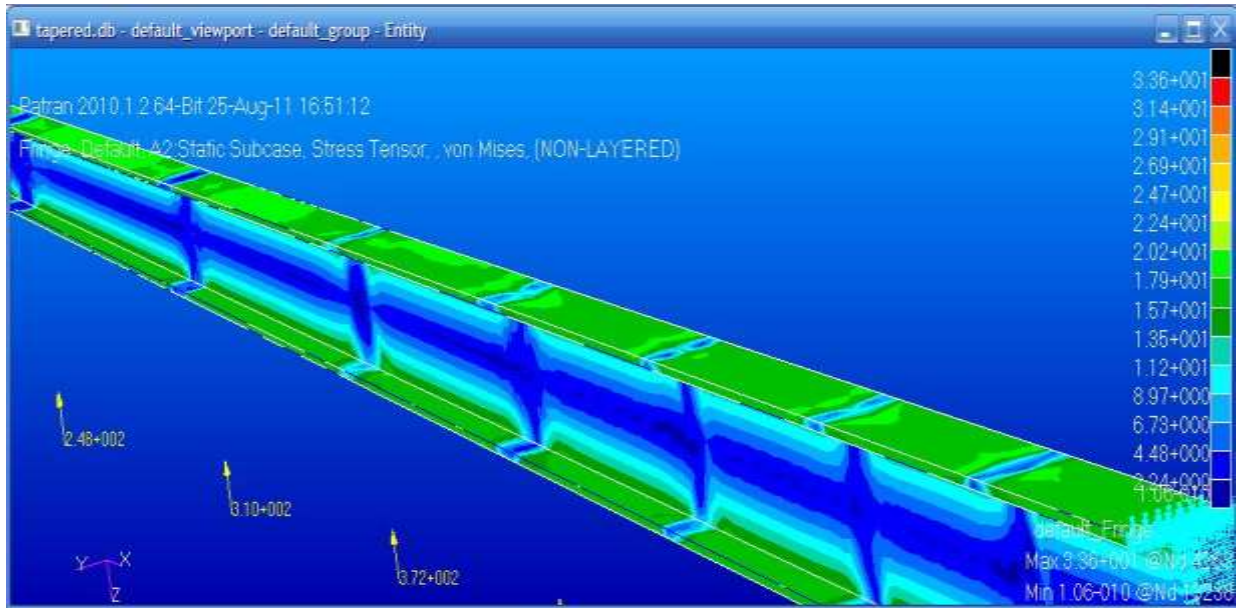


Fig. 5.4 Detailed View

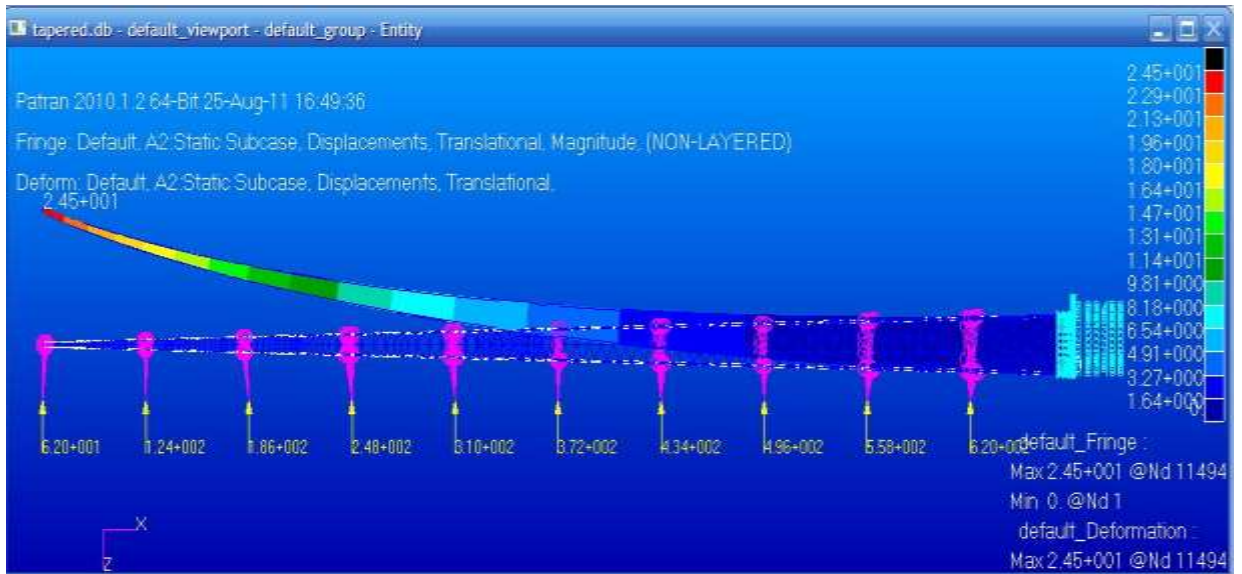


Fig. 5.5 Displacement results for Tapered Spar Beam with $t = 8.205\text{mm}$

Mass of the Tapered Spar Beam = 8.393 kg.

- **Iteration 2: $t=6.2\text{mm}$**

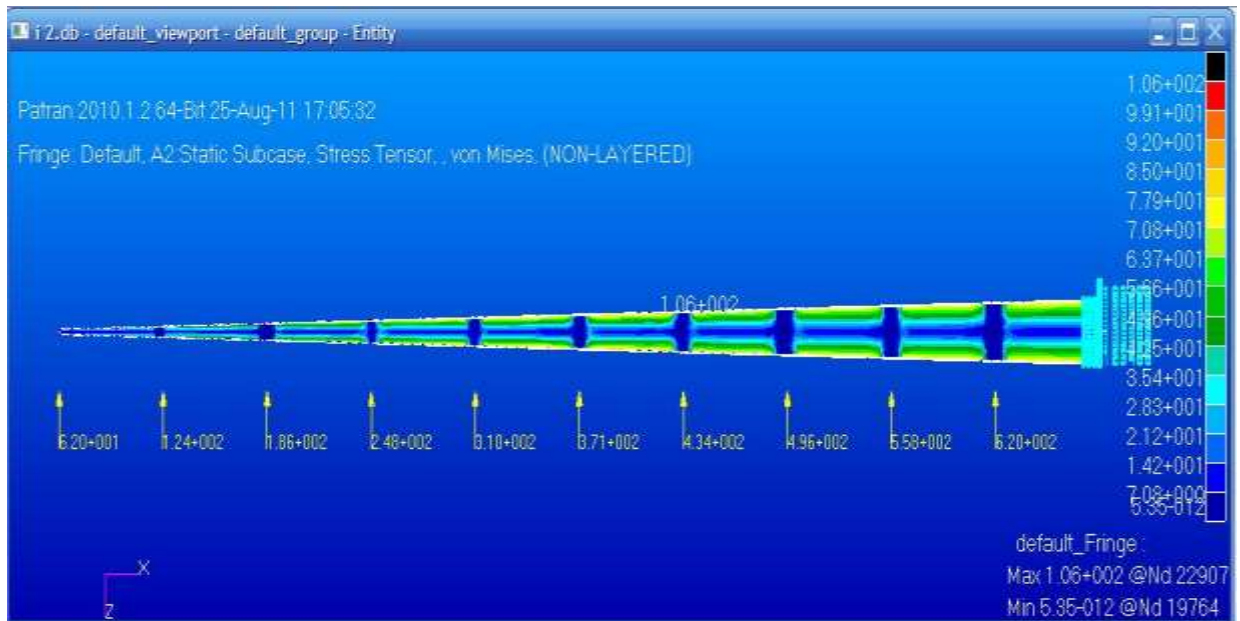


Fig. 5.6 Stress Distribution Contour of Tapered Spar Beam with $t = 6.2\text{mm}$

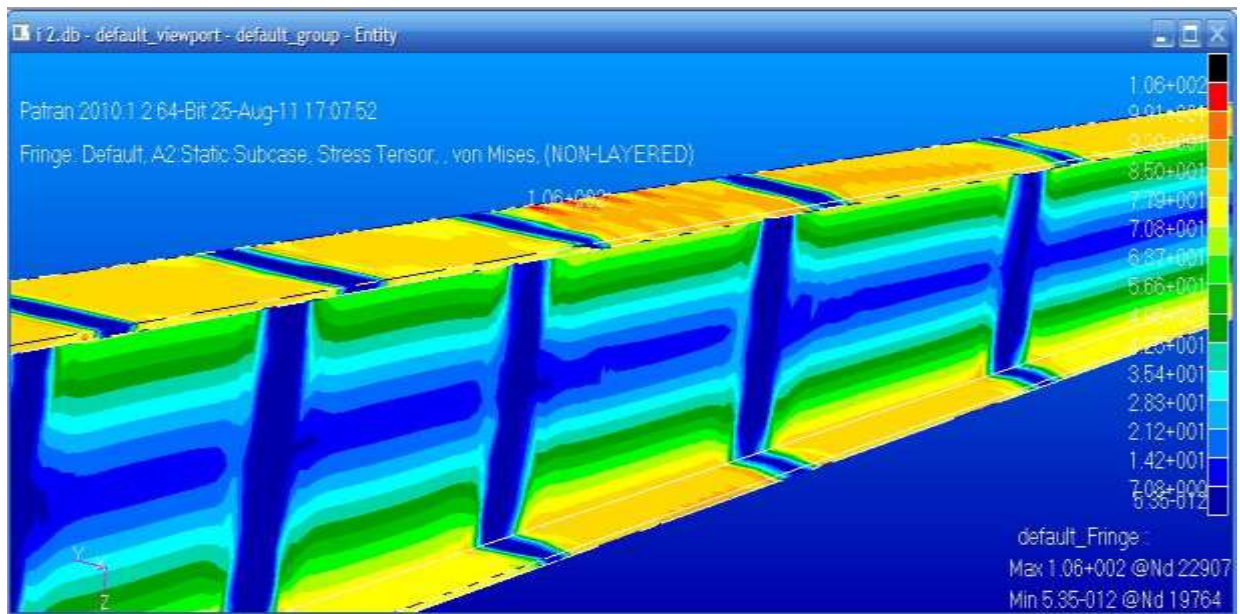


Fig. 5.7 Maximum Stress Region

After applying loads (as shown in Fig. 5.6) and boundary condition, maximum stress value is found to be 106 MPa which is again much less than the yield strength of the material. Therefore, this case is valid for the design of spar beam.

Hence, the third iteration will be carried out for further reduced thickness.

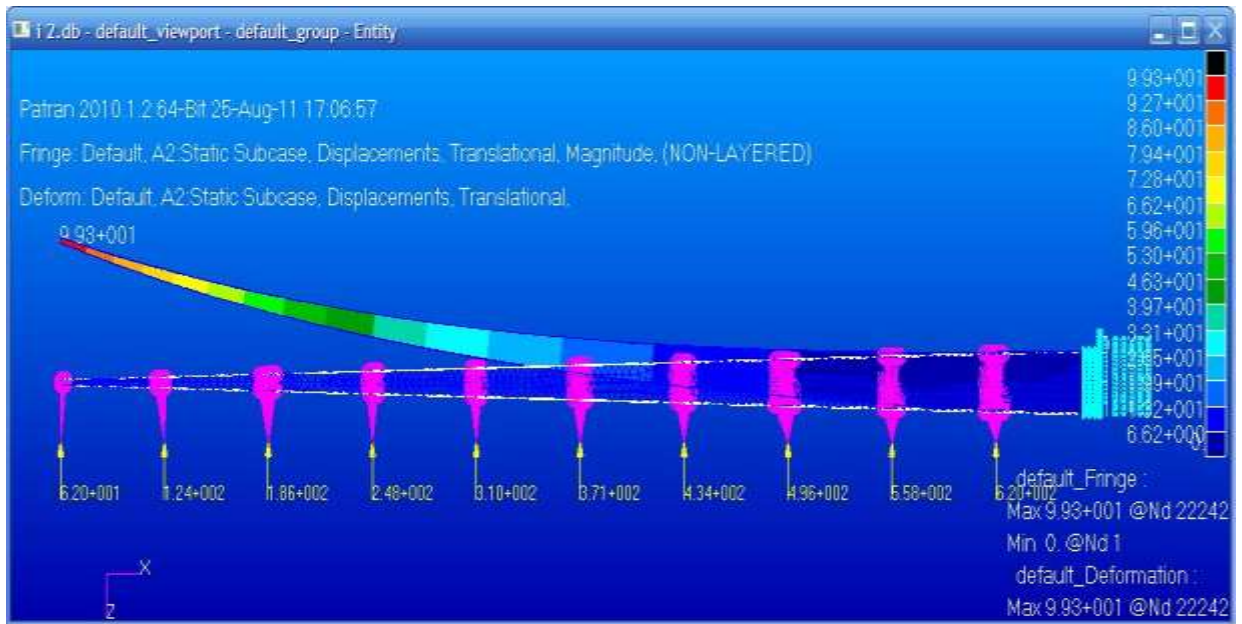


Fig. 5.8 Displacement results for Tapered Spar Beam with $t = 6.2\text{mm}$

Initial Mass of the Tapered Spar Beam ($t = 8.205\text{ mm}$) = 8.393 kg.

Final Mass of the Tapered Spar Beam ($t = 6.2\text{ mm}$) = 3.611 kg.

- **Iteration 3: $t=3.5\text{mm}$**

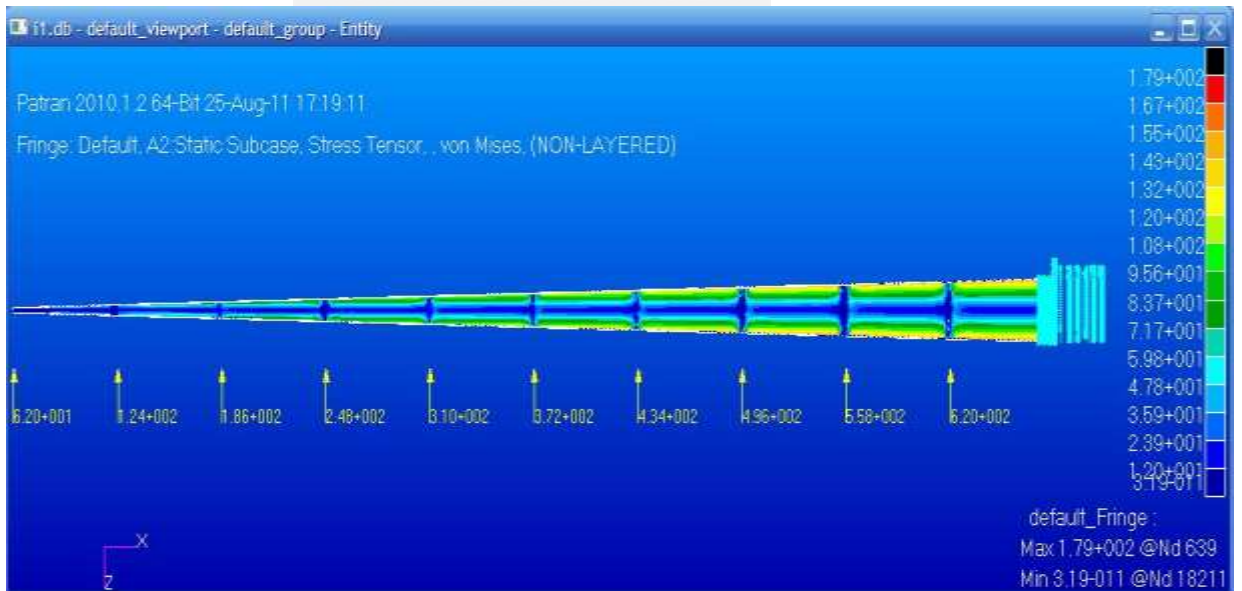


Fig. 5.9 Stress Distribution Contour of Tapered Spar Beam with $t = 3.5\text{mm}$

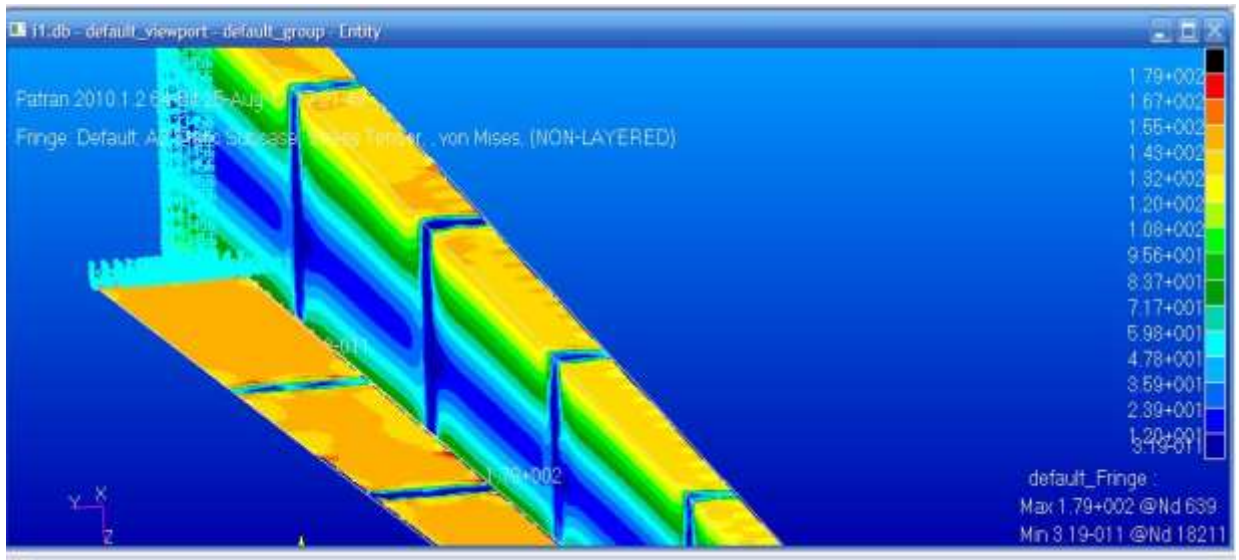


Fig. 5.10 Maximum Stress Region

After applying loads (as shown in Fig. 5.9) and boundary condition, maximum stress value is found to be 179 MPa which is again much less than the yield strength of the material. Therefore, this case is valid for design of spar beam.

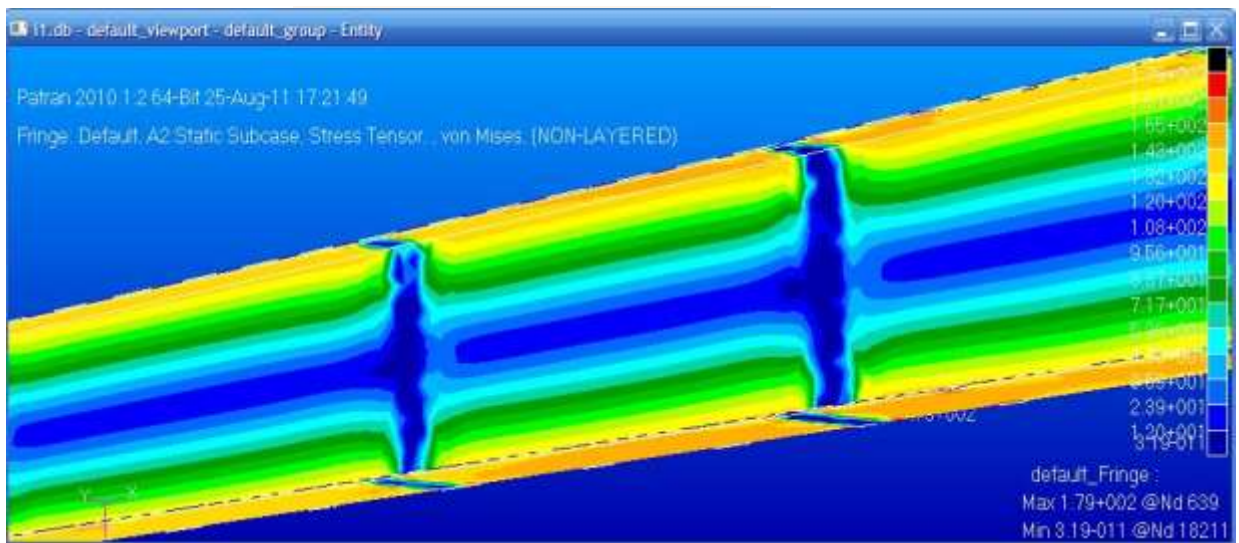


Fig. 5.11 Detailed View

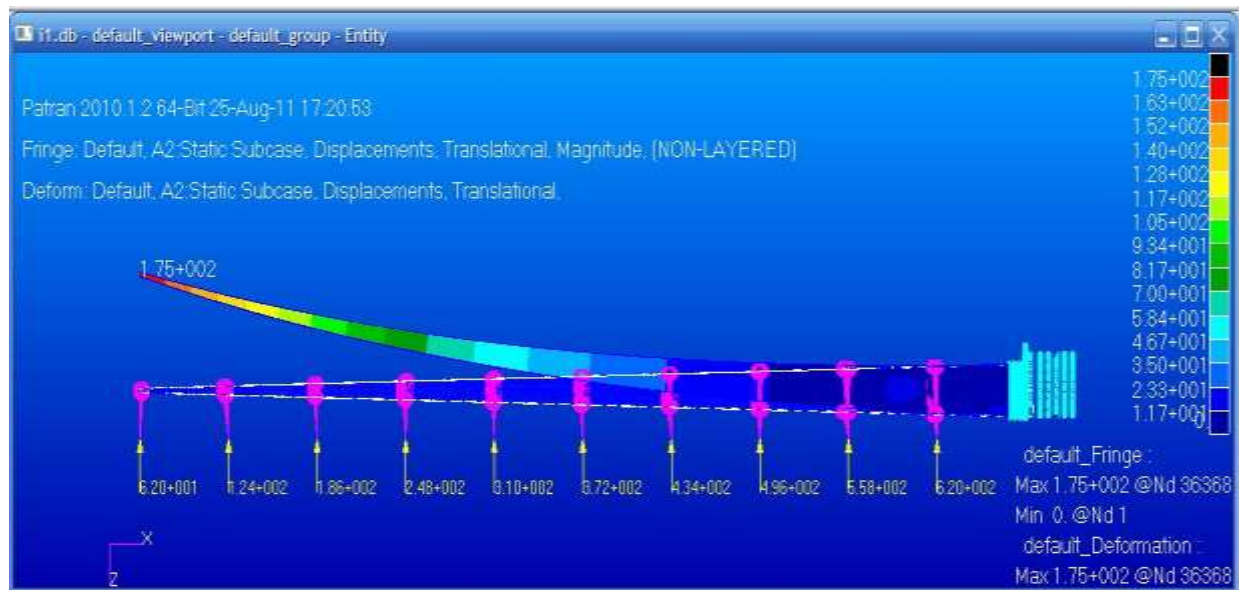


Fig. 5.12 Displacement results for Tapered Spar Beam with $t = 3.5\text{mm}$

Initial Mass of the Tapered Spar Beam ($t = 8.205\text{ mm}$) = 8.393 kg.

Final Mass of the Tapered Spar Beam ($t = 3.5\text{ mm}$) = 2.118 kg.

5.2.2 Cutouts Iteration

Cutouts are essential in airframe structures to provide the following:

- Holes in webs are frequently used to save structural weight.
- Passages for wire bundles, control linkages, etc.
- Accessibility for final assembly and maintenance.
- Inspection for maintenance.
- Elliptical cutouts are a simple and lower cost method for fabricating access holes. Elliptical holes are typically used for crawl holes in empennage applications.

Cutouts in shear beams (shear load in web):

- Lightly loaded beams (e.g., ribs, formers, etc.)
- Moderately loaded beams (e.g., control surface box spars, auxiliary spars, etc.)
- Heavily loaded beams (e.g., wing and empennage spars, etc.)

Cutout Analysis Methods

- No clear-cut analytical procedure for sizing cutouts is available.

- With the help of existing test data and empirical reports an experienced engineer can select acceptable proportions.
- Doubtful cases should be tested.
- There is still not sufficient test data available for the sizing of various cutouts in airframe structures and extensive test programs are required to substantiate cutout analysis methods for new aircraft programs.

Vertical Cutouts Iterations:

The schematic cutout dimensions are shown.

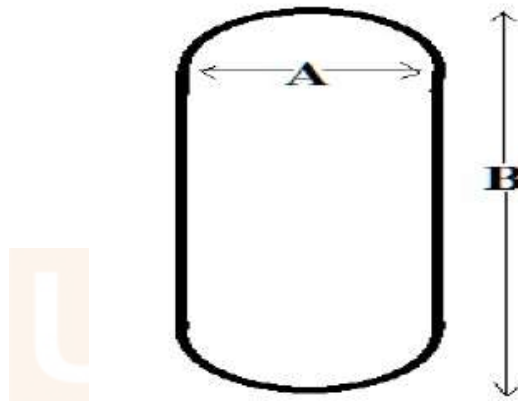


Fig. 5.13 Cutout Model

According to the Table 5.1 cutouts are introduced into the spar beam web, loads and boundary condition are applied to find out the stresses in each station. If stresses are lower than the ultimate strength value, the design is valid. The spar beam with the cutout dimensions are shown in Table 5.1.

Table 5.1 Dimensions of Vertical Cut-outs

Section	B (mm)	A (mm)
0-1	70	50
1-2	65	47.5
2-3	60	45
3-4	55	42.5
4-5	50	40
5-6	40	35
6-7	35	30
7-8	25	20

8-9	15	12
9-10	8	6

The spar beam with the cutout dimensions are shown in Table. It is geometrically represented below. CATIA V5 software is used to draw this model. This model is used for further analysis in NASTRAN and PATRAN software.

- **Iteration 1: $t=6.2\text{mm}$**

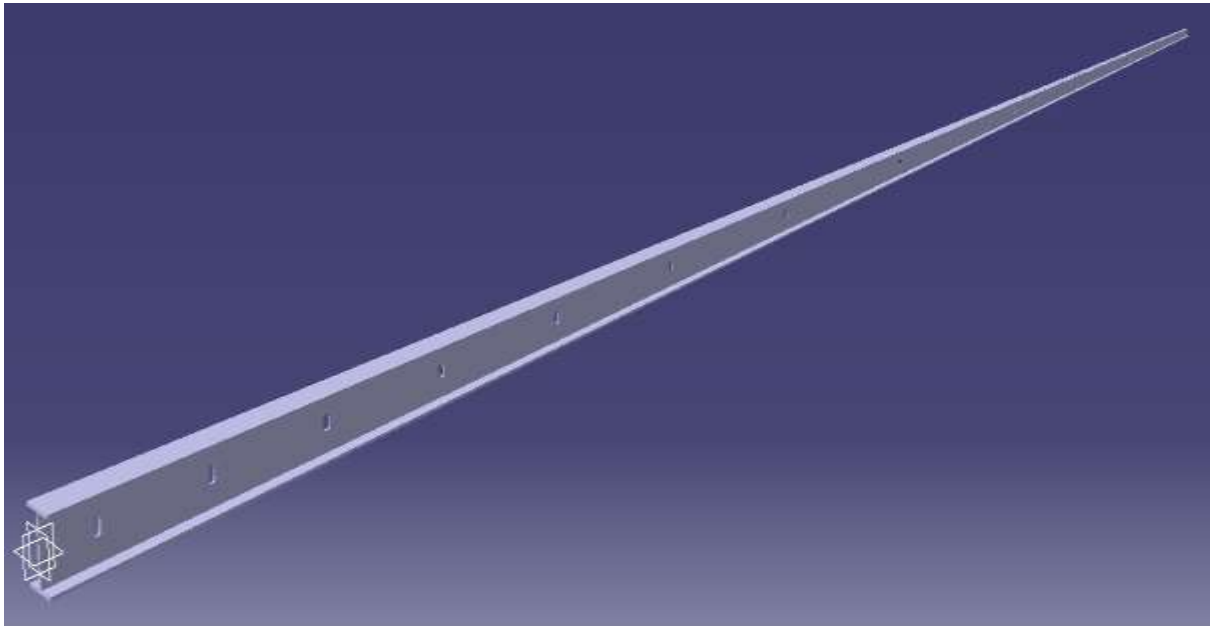


Fig. 5.14 Isometric view of Tapered Spar Beam with Cut-outs



Fig. 5.15 Side View of Tapered Spar Beam with Cut-outs

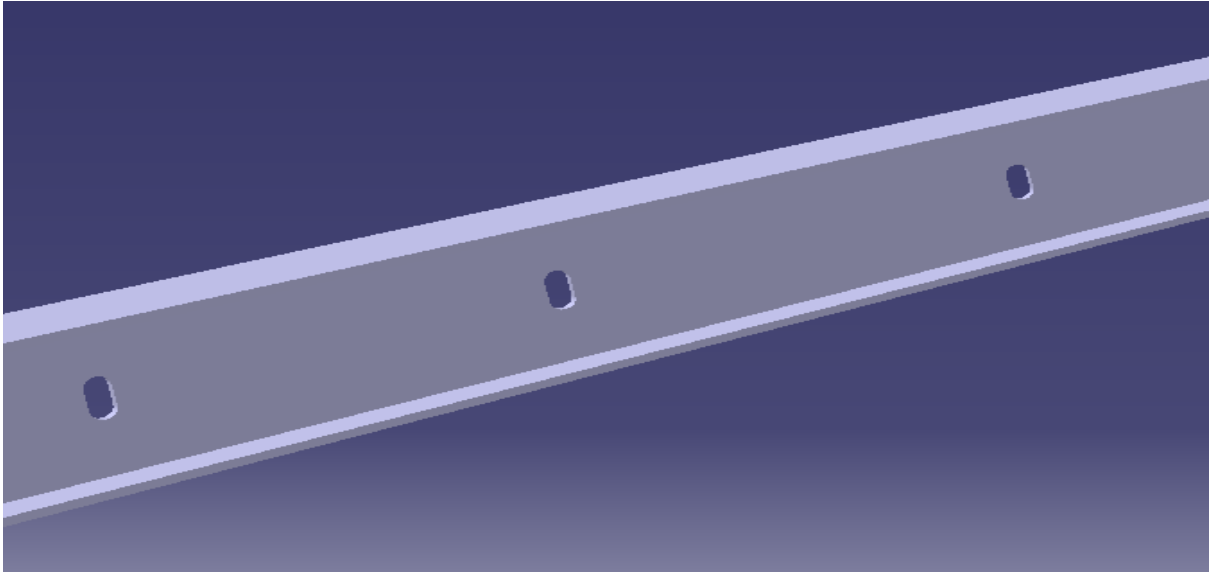


Fig. 5.16 Close View of Tapered Spar Beam with Cut-outs

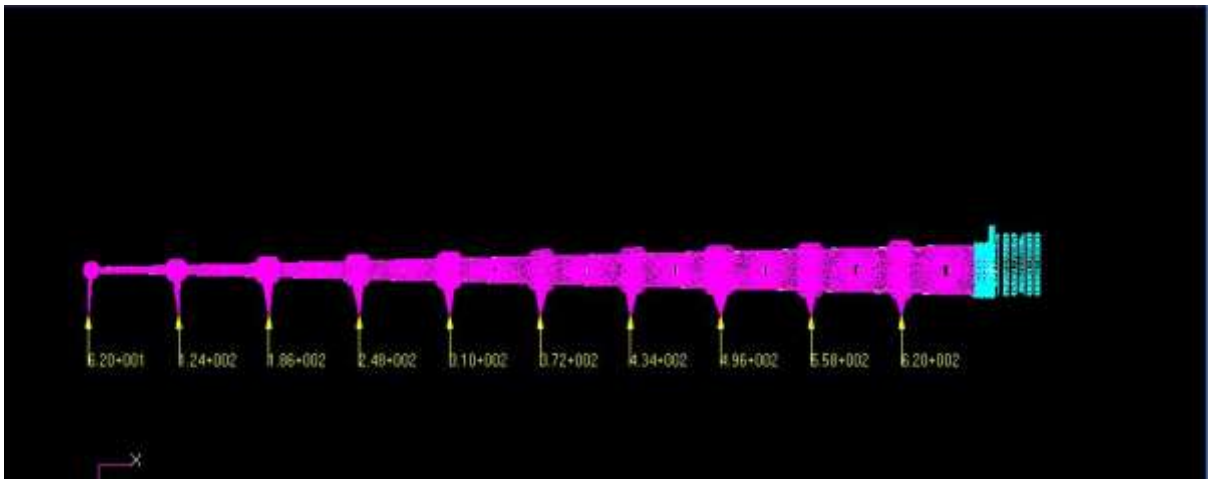


Fig. 5.17 Mesh Model of Tapered Spar Beam with Cut-outs

Stress distribution contour is shown below.

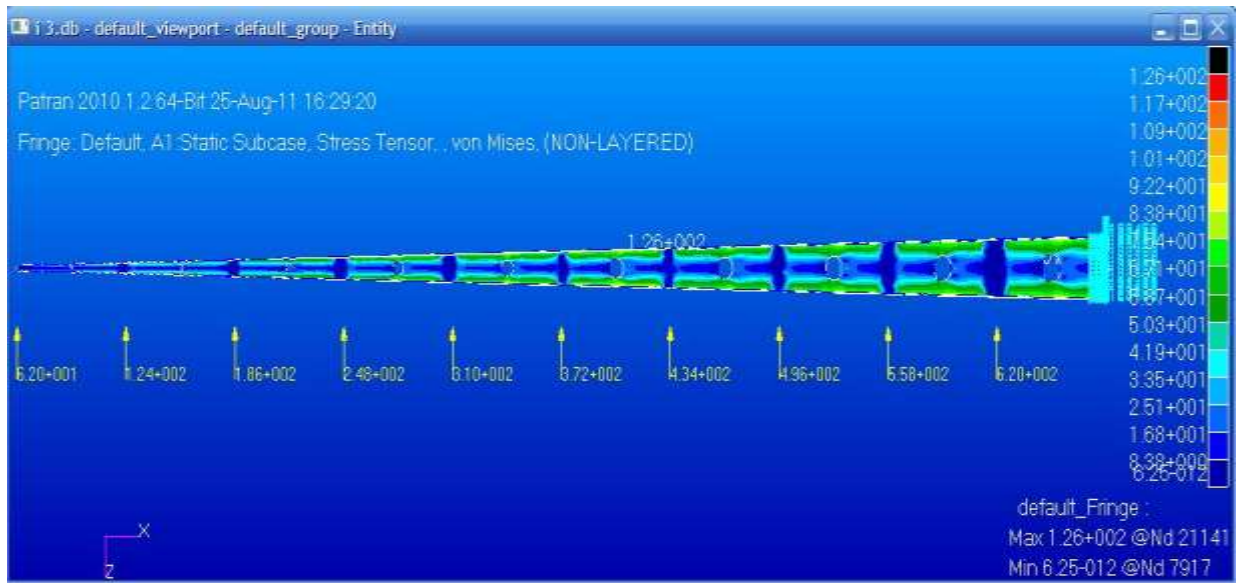


Fig. 5.18 Stress Distribution Contour of Tapered Spar Beam with Vertical Cut-outs for $t = 6.2\text{mm}$

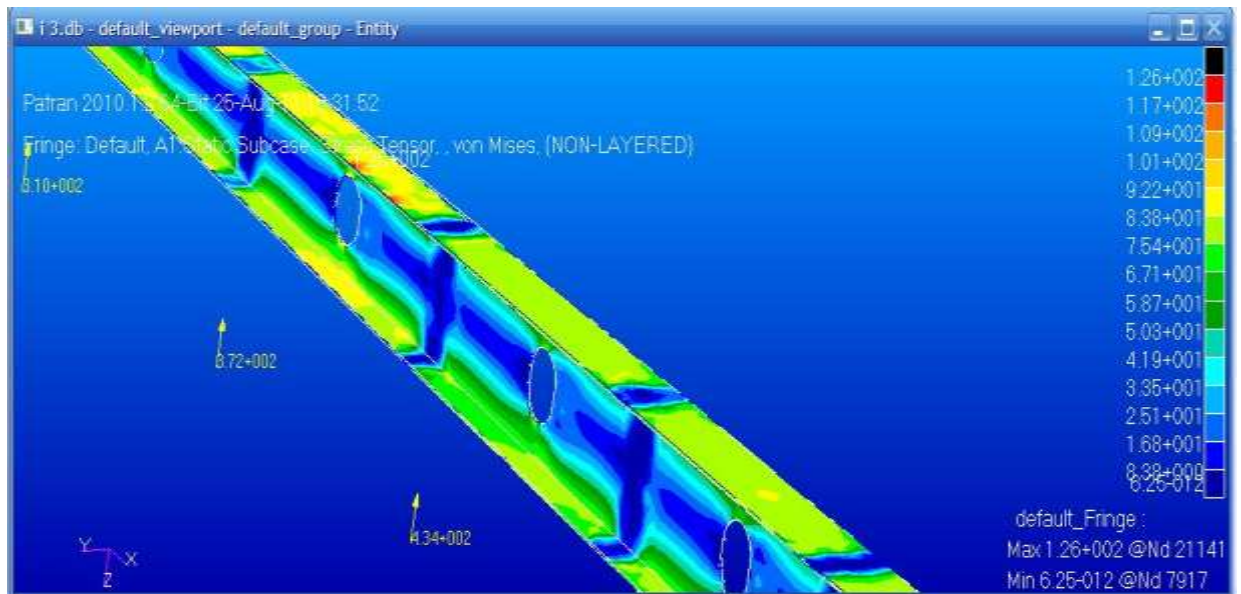


Fig. 5.19 Maximum Stress Region

After applying loads (as shown in Fig 5.18) and boundary condition, maximum stress value is found to be 126 MPa which is much less than the yield strength of the material. Therefore, this case is valid for the design of spar beam.

Hence, the second iteration will be carried out for further reduced thickness for same cutouts.

Design and Analysis of A Spar Beam for Vertical Tail of a Transport Aircraft.

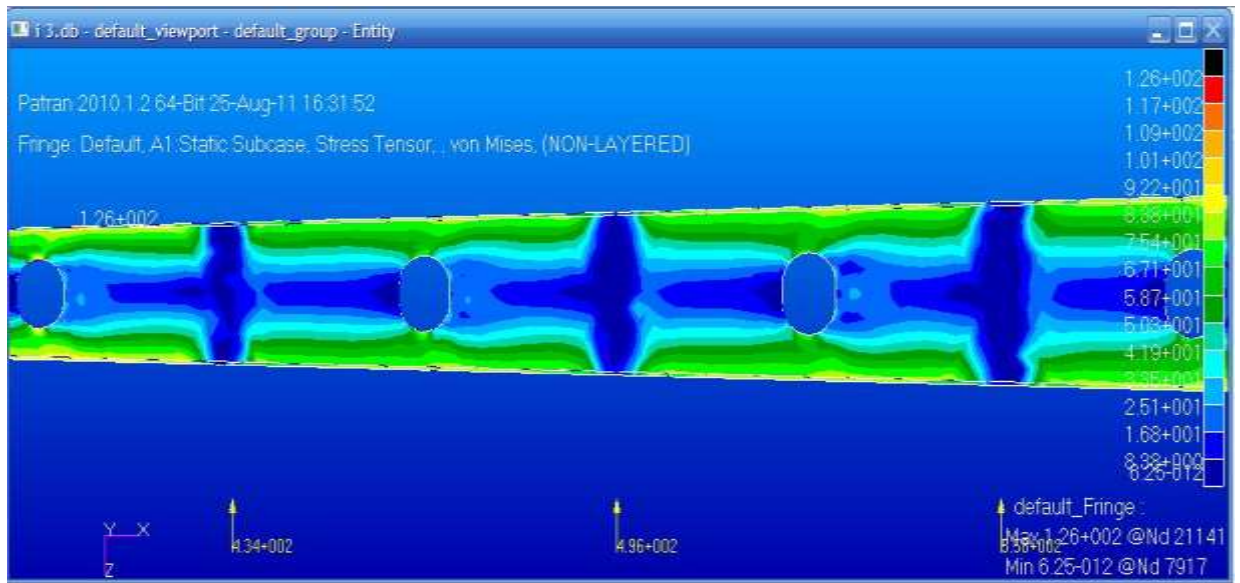


Fig. 5.20 Detailed View

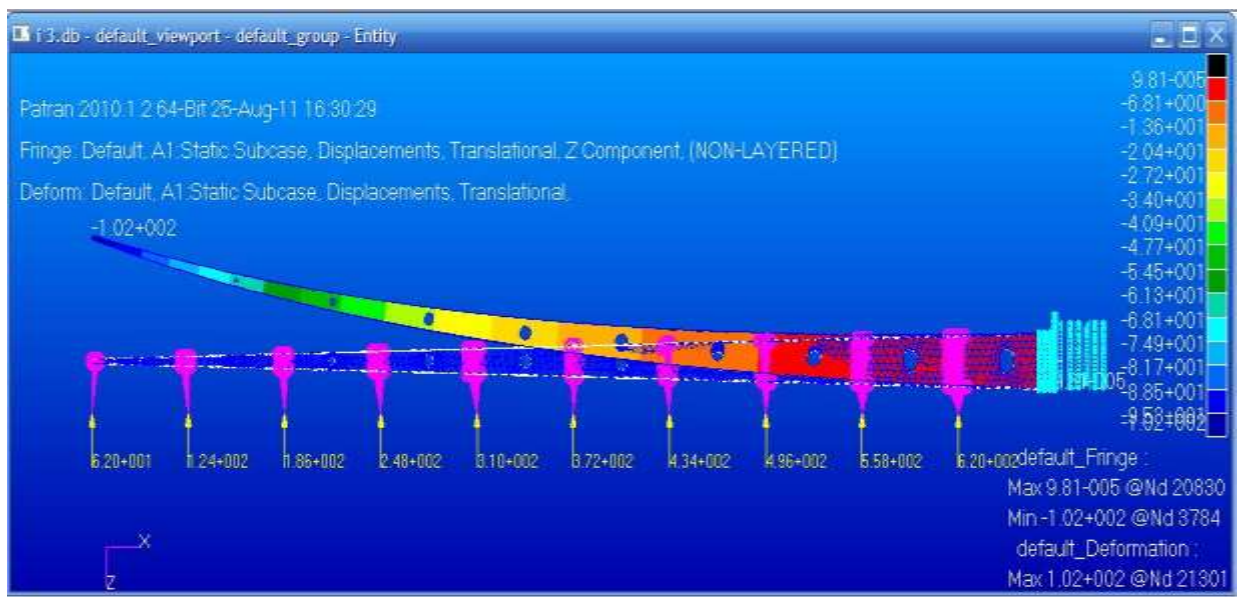


Fig. 5.21 Displacement results for Tapered Spar Beam with Vertical Cut-outs for $t = 6.2\text{mm}$

Initial Mass of the Tapered Spar Beam ($t = 6.2\text{ mm}$) = 3.611 kg.

Final Mass of the Tapered Spar Beam with Vertical Cut-outs ($t = 6.2\text{ mm}$) = 3.202 kg.

- **Iteration 2: $t=3.5$ mm**

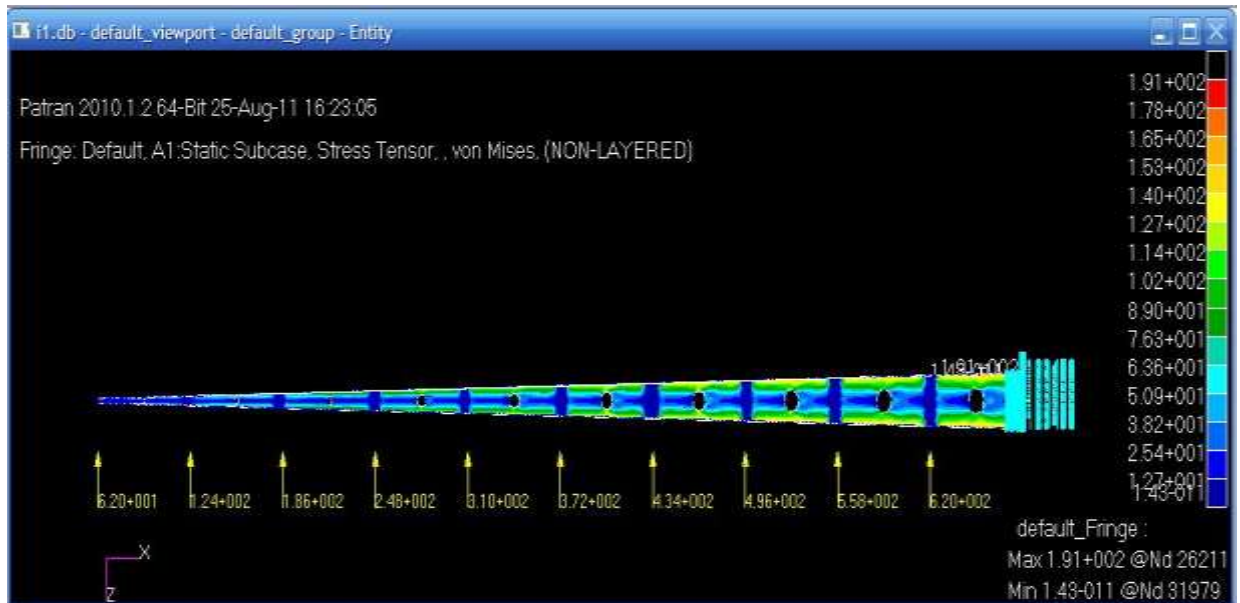


Fig. 5.22 Stress Distribution Contour of Tapered Spar Beam with Vertical Cut-outs for $t = 3.5$ mm

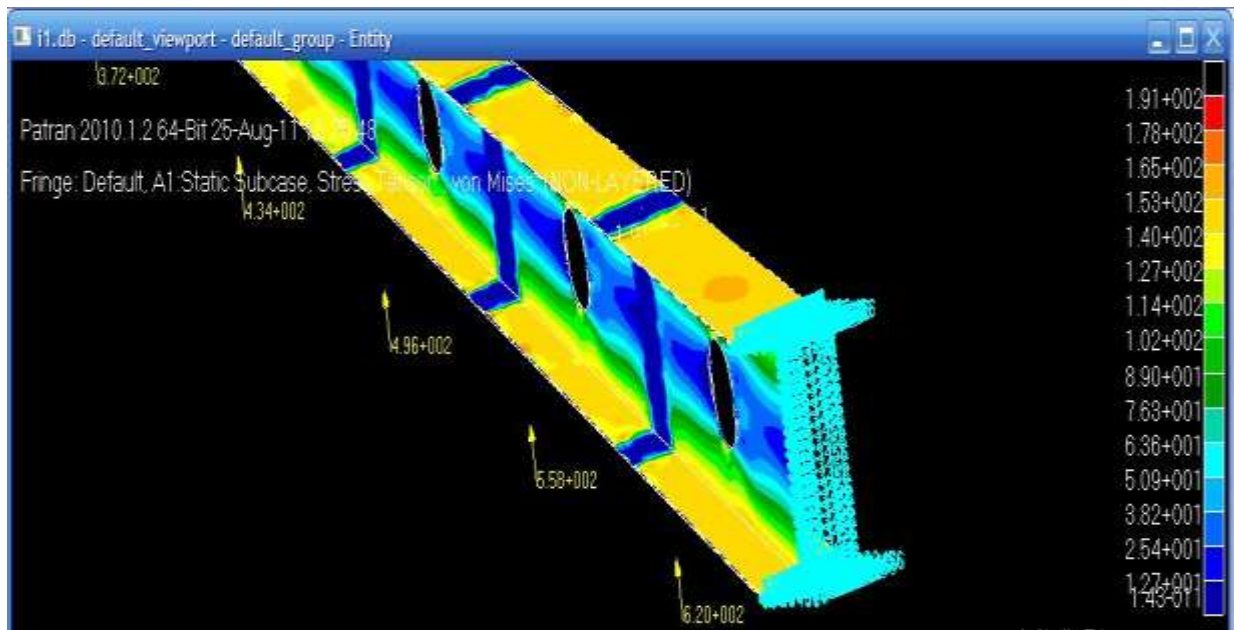


Fig. 5.23 Maximum Stress Region

After applying loads (as shown in Fig 5.22) and boundary condition, maximum stress value is 191 MPa which is again less than the yield strength of the material. Therefore, this case is valid for the design of spar beam.

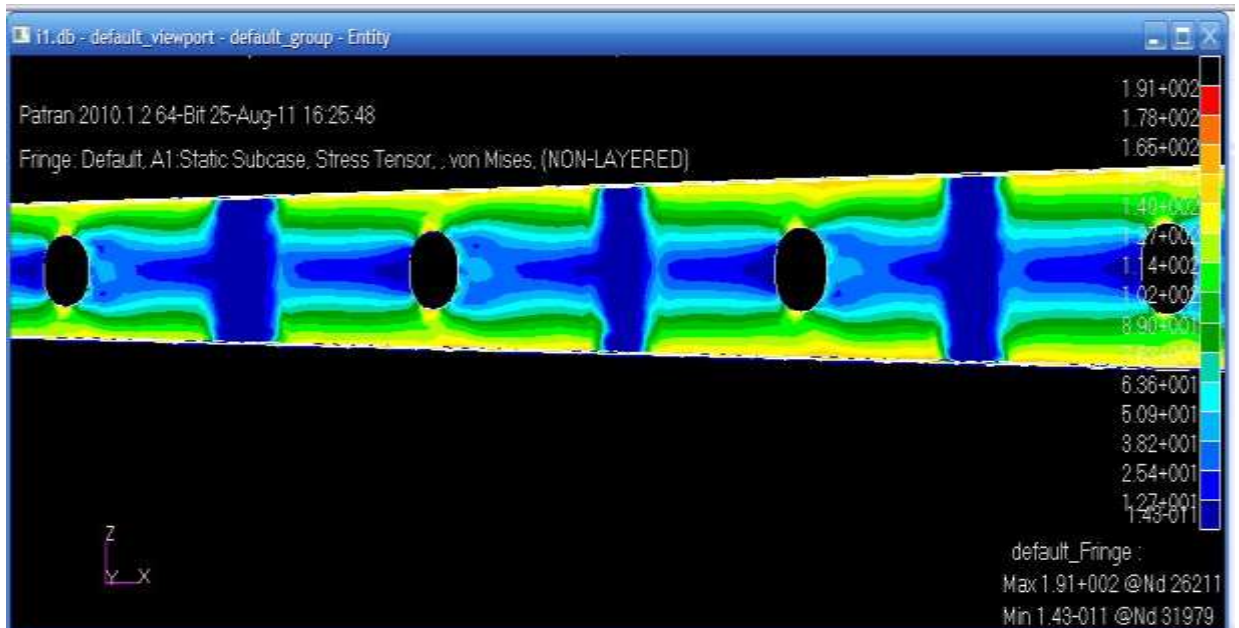


Fig. 5.24 Detailed View

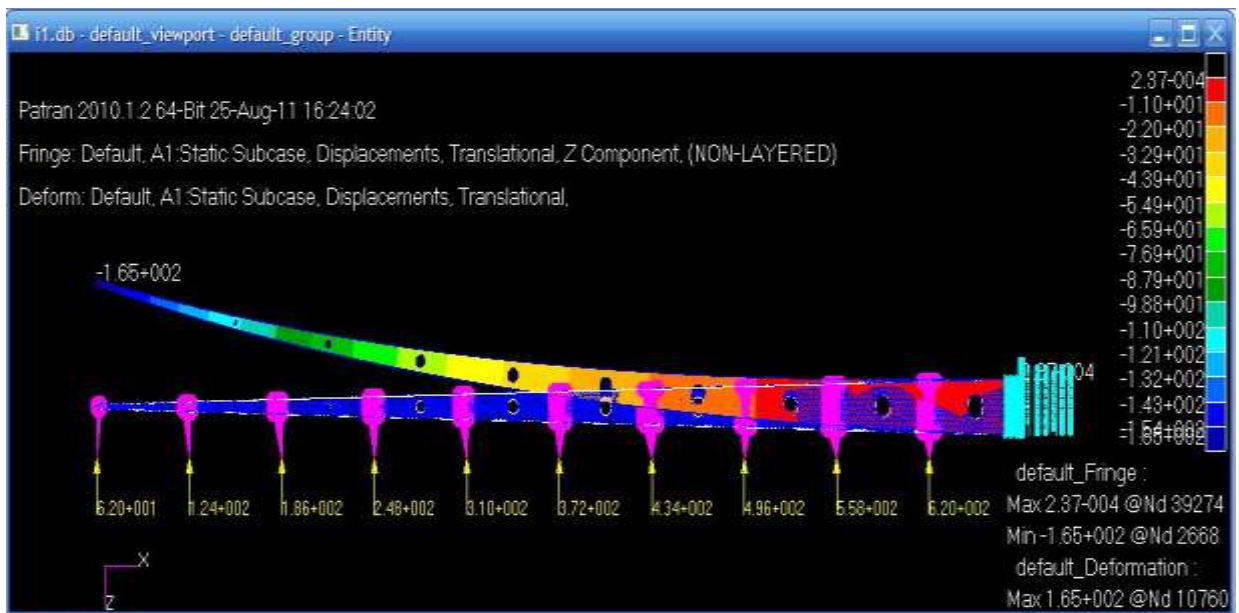


Fig. 5.25 Displacement results for Tapered Spar Beam with Vertical Cut-outs for $t = 3.5\text{ mm}$

Initial Mass of the Tapered Spar Beam ($t = 3.5\text{ mm}$) = 2.118 kg

Final Mass of the Tapered Spar Beam with Vertical Cut-outs($t = 3.5\text{ mm}$) = 2.01 kg

Horizontal Cutouts Iterations

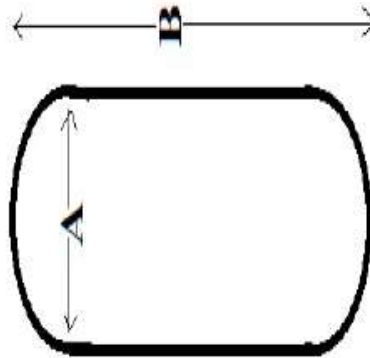


Fig. 5.26 Cutout Model

Table 5.2 Dimensions of Horizontal Cut-outs

Section	B (mm)	A (mm)
0-1	200	60
1-2	200	55
2-3	200	50
3-4	200	45
4-5	200	40
5-6	200	35
6-7	200	30
7-8	200	20
8-9	200	15
9-10	200	5

- **Iteration 3: $t=6.2$ mm**

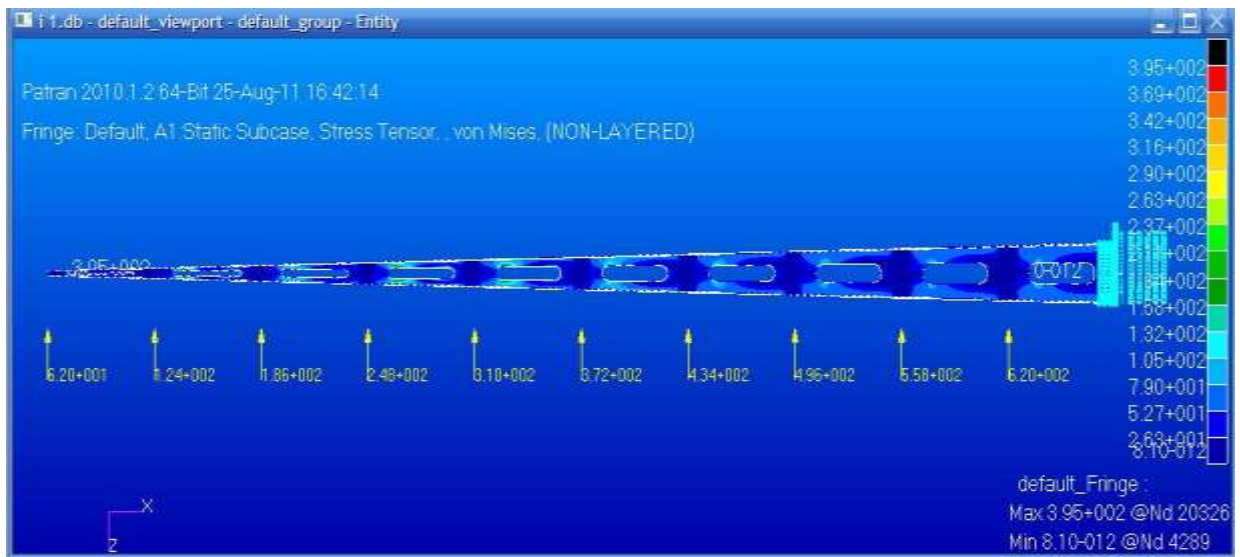


Fig. 5.27 Stress Distribution Contour of Tapered Spar Beam with Horizontal Cut-outs for $t = 6.2$ mm

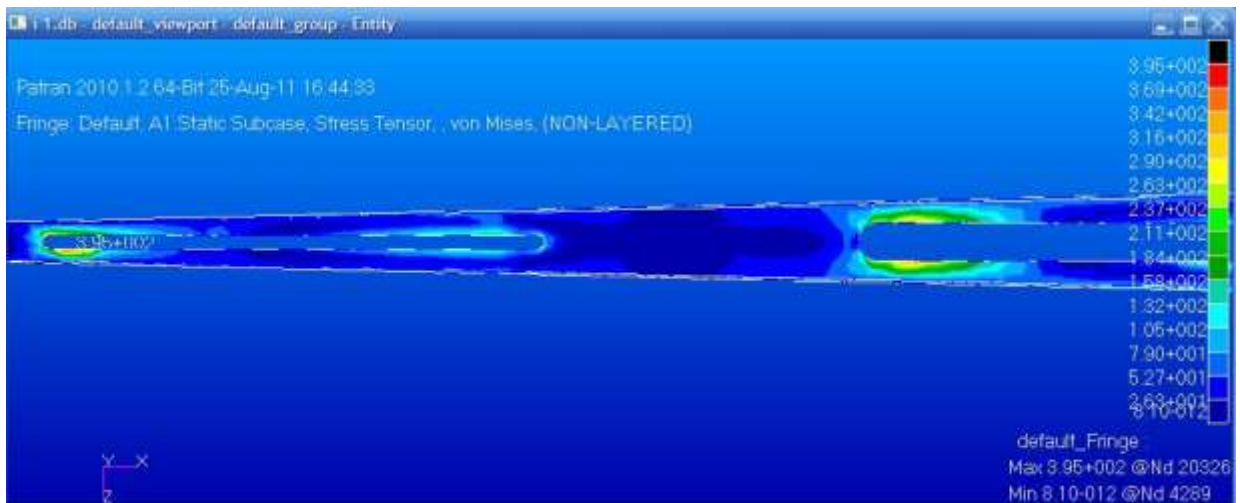


Fig. 5.28 Maximum Stress Region

After applying loads (as shown in Fig 5.27) and boundary condition, maximum stress value is 200 MPa which is again less than the yield strength of the material. Therefore, this case is valid for the design of spar beam.

Hence, the fourth iteration will be carried out for further reduced thickness for same cutouts.

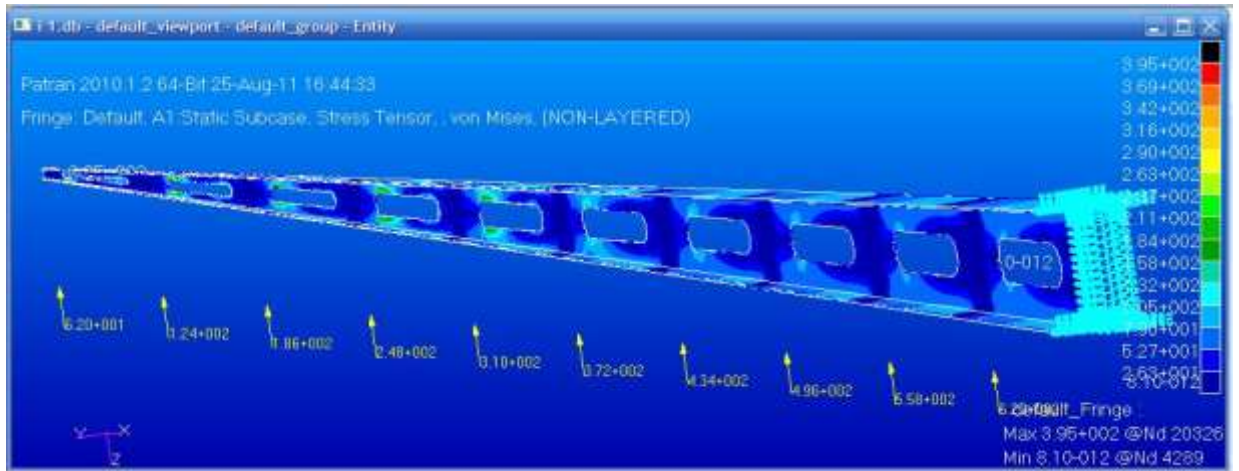


Fig. 5.29 Detailed View

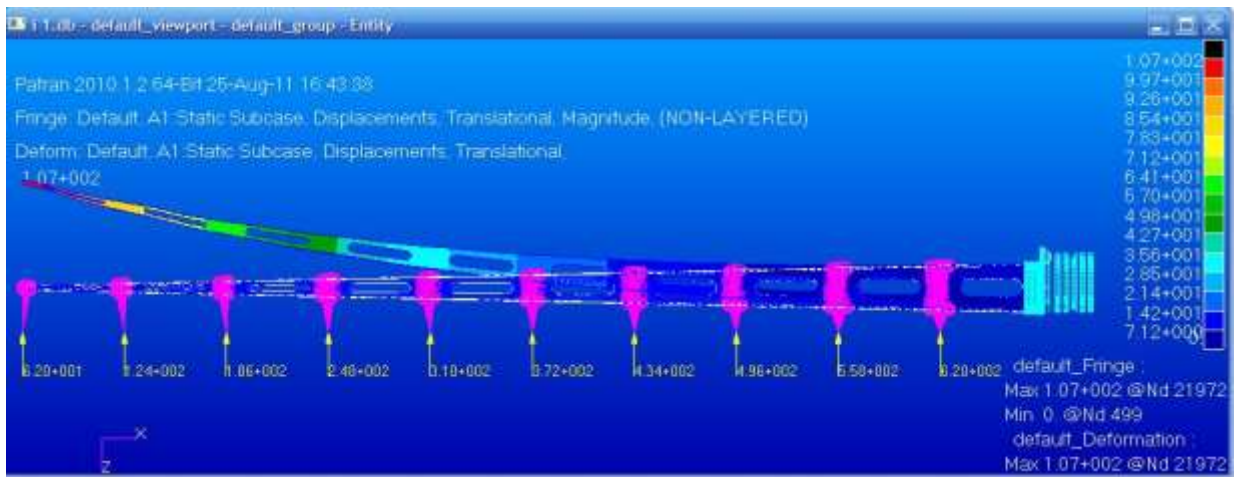


Fig. 5.30 Displacement results for Tapered Spar Beam with Horizontal Cut-outs for $t = 6.2\text{mm}$

- **Iteration 4: $t=3.5\text{ mm}$**

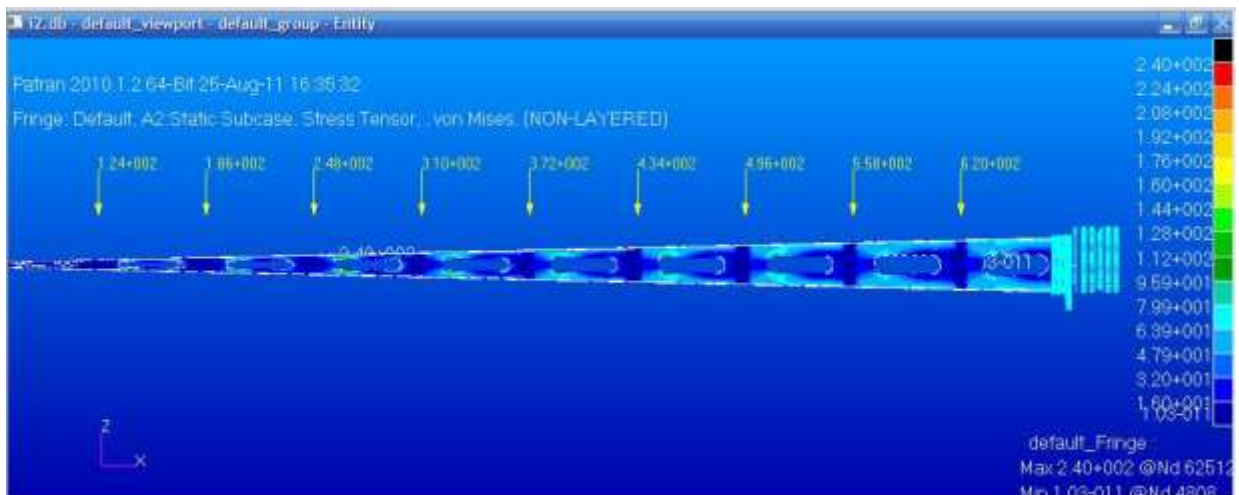


Fig. 5.31 Stress Distribution Contour of Tapered Spar Beam with Horizontal Cut-outs for $t = 3.5\text{mm}$

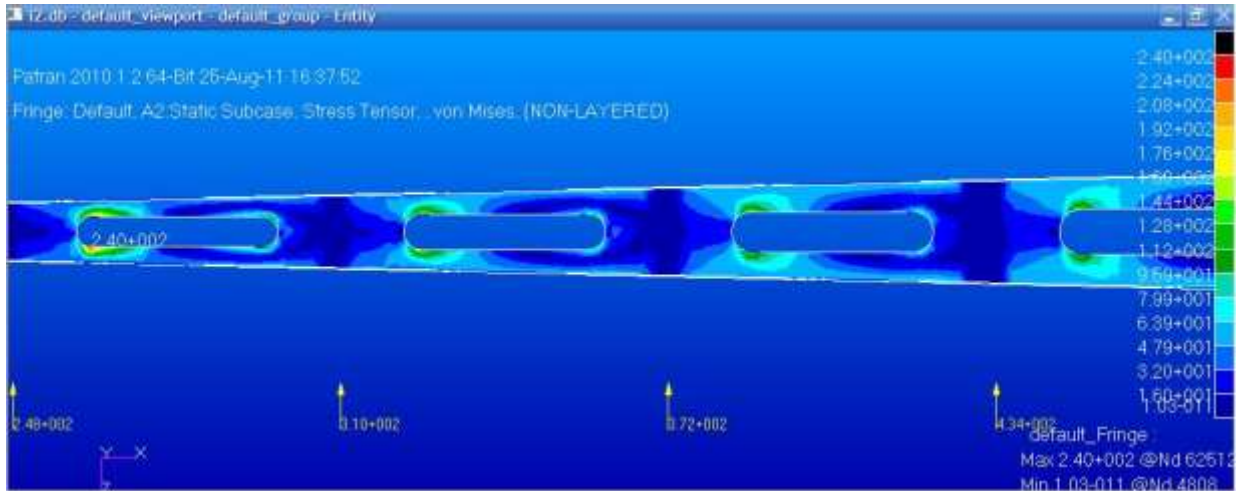


Fig. 5.32 Maximum Stress Region

After applying loads (as shown in Fig 5.31) and boundary condition, maximum stress value is 240 MPa which is again less than the yield strength of the material. Therefore, this case is valid for the design of spar beam.

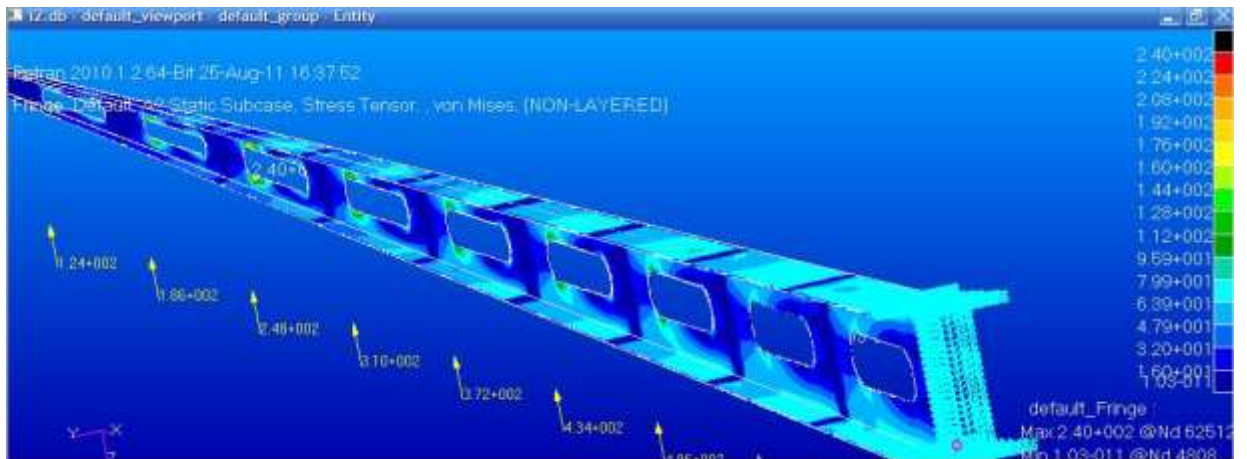


Fig. 5.33 Detailed View

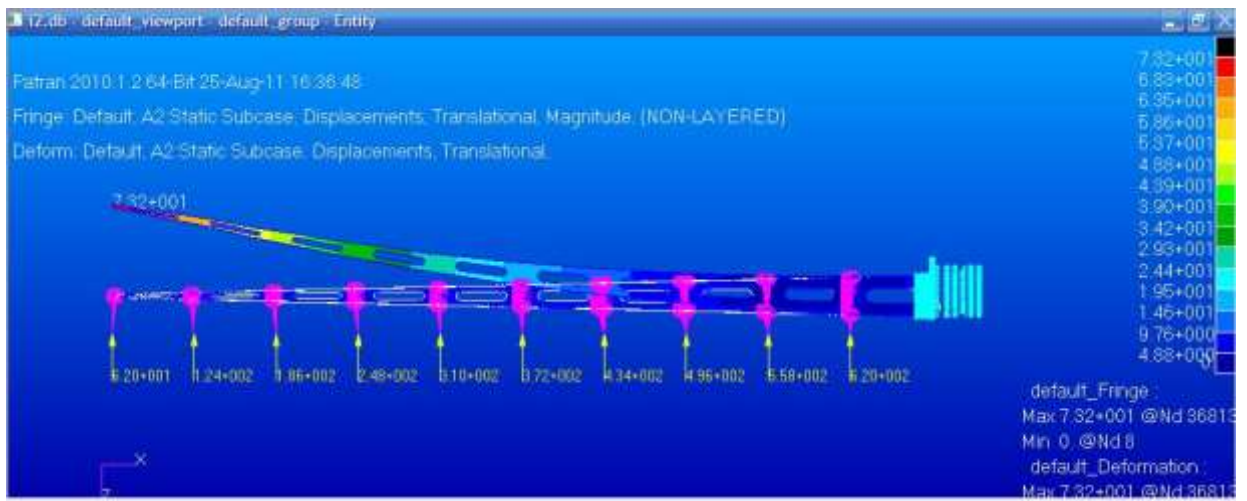


Fig. 5.34 Displacement results for Tapered Spar Beam with Horizontal Cut-outs for $t = 3.5\text{mm}$

Mixed Cutouts with $t = 3.5$



Fig. 5.35 Side View of Tapered Spar Beam with Mixed Cut-outs

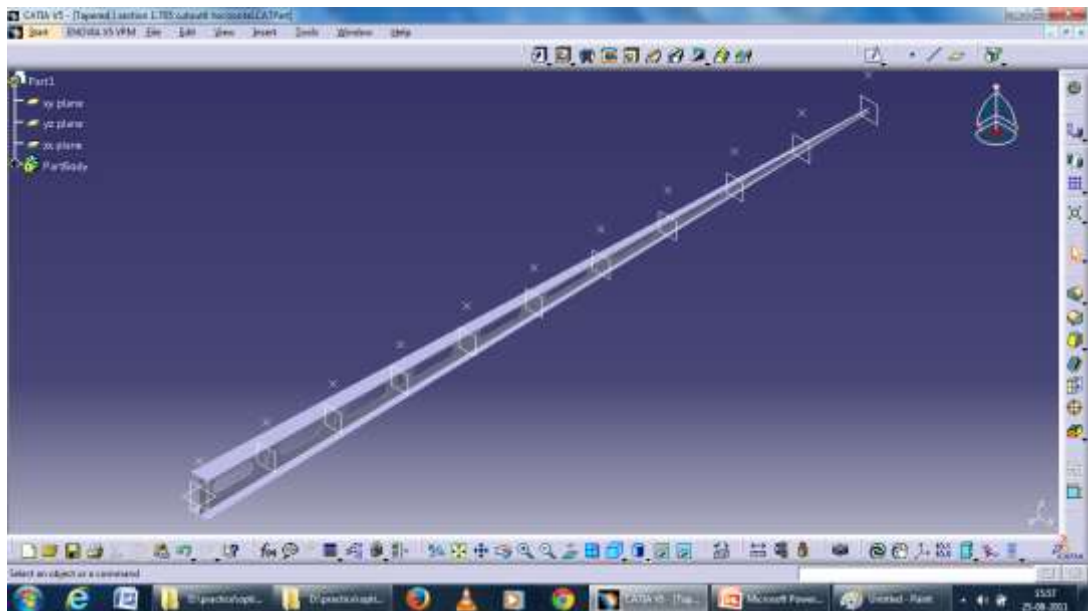


Fig. 5.36 Isometric view of Tapered Spar Beam with Cut-outs

- **Iteration 5:**

In this iteration, we will introduce horizontal cutouts in all 10 sections and vertical cutouts at first 6 stations starting from the fixed end.

Table 5.3 Dimensions of Horizontal Cut-outs

Section	B (mm)	A (mm)
0-1	200	60
1-2	200	55
2-3	200	50
3-4	200	45
4-5	200	40
5-6	200	35
6-7	200	30
7-8	200	20
8-9	200	15
9-10	200	5

Table 5.4 Dimensions of Vertical Cutouts

Station	B (mm)	A (mm)
1	25	44
2	22.5	40
3	20	35
4	17.5	31
5	15	26
6	12.5	22.4

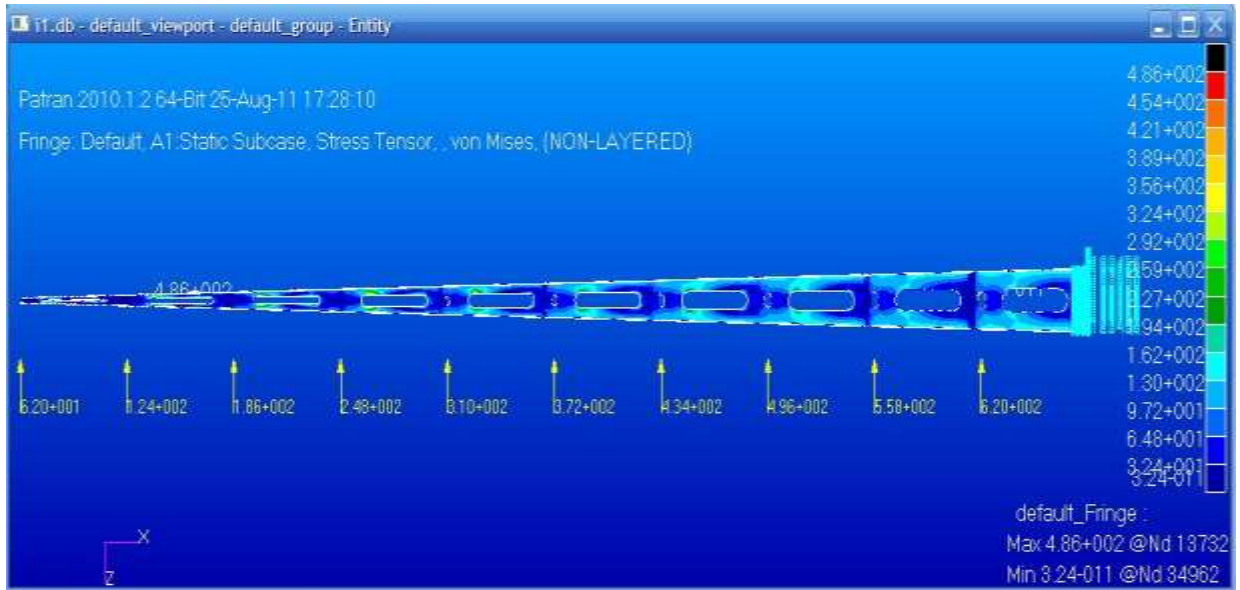


Fig. 5.37 Stress Distribution Contour of Tapered Spar Beam with 10 Horizontal Cut-outs & 6 Vertical Cutouts

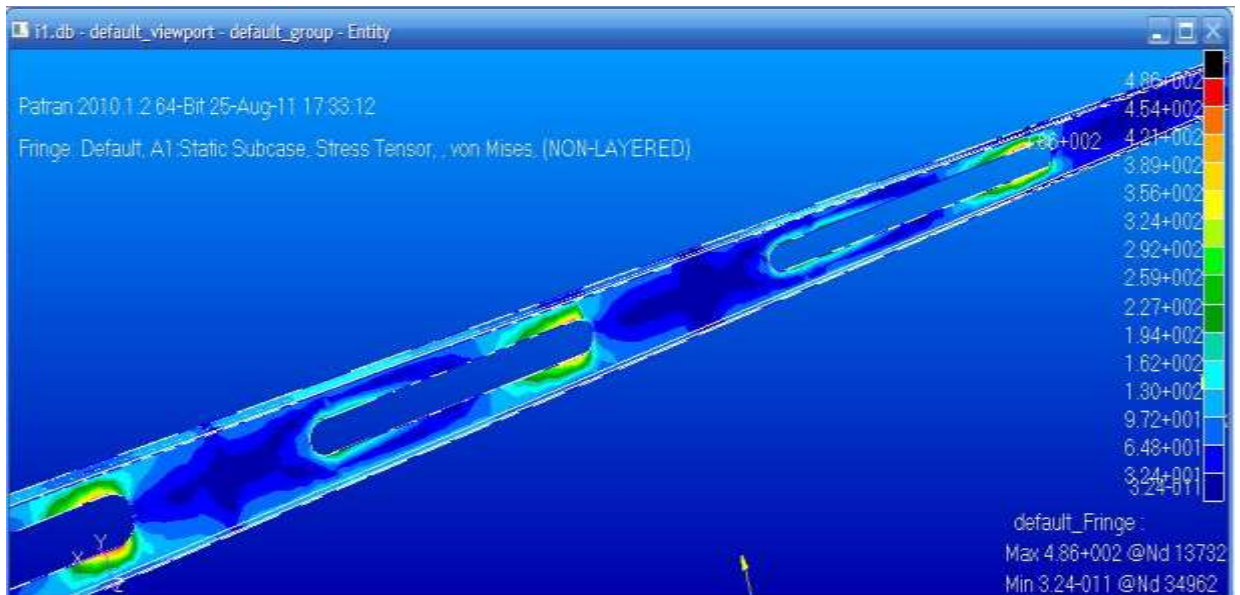


Fig. 5.38 Maximum Stress Region

After applying loads (as shown in Fig) and boundary condition, maximum stress value is 486 MPa which is much greater than the yield strength of the material. Hence this case is not valid for design of spar beam.

Hence, we will reduce the number of cutouts in the next iteration.

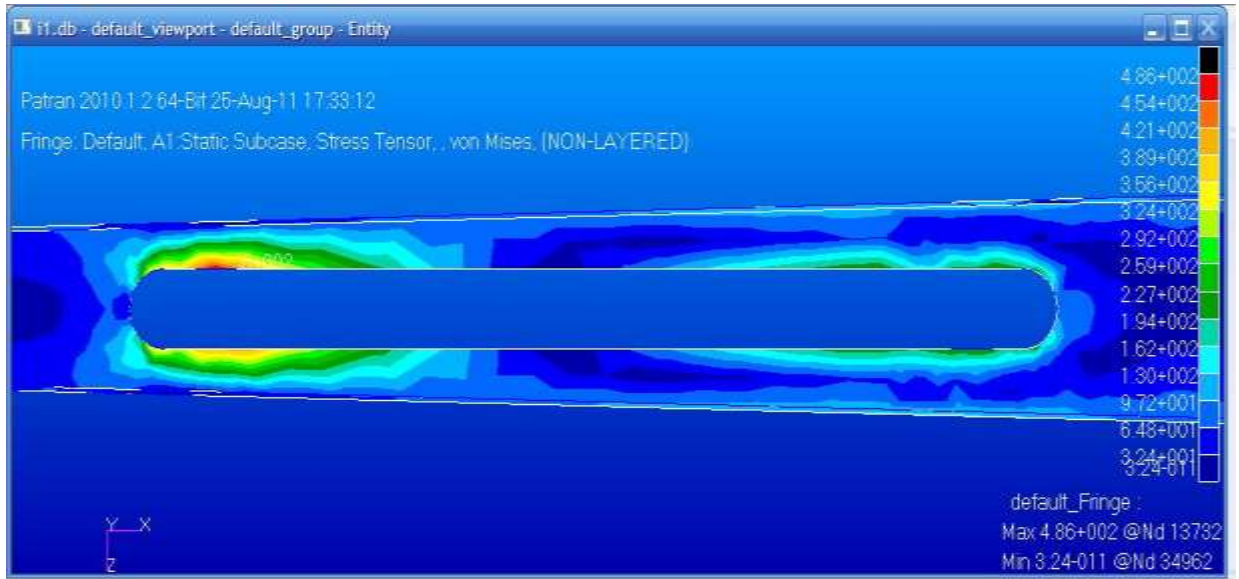


Fig. 5.39 Detailed View

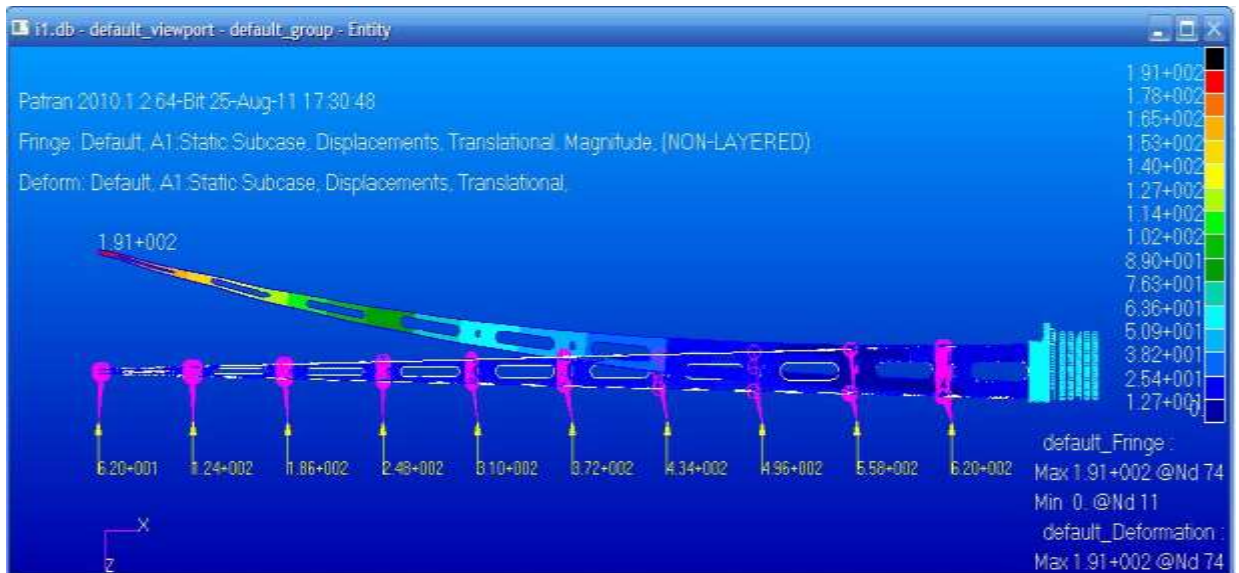


Fig. 5.40 Displacement Results for Tapered Spar Beam with 10 Horizontal Cut-outs & 6 Vertical Cutouts

- **Iteration 6:**

In this iteration, we will introduce horizontal cutouts in all 10 sections and vertical cutouts at first 3 stations starting from the fixed end. But the second last horizontal cutout will be smaller in size than in earlier case.

Table 5.5 Dimensions of Horizontal Cut-outs

Section	B (mm)	A (mm)
0-1	200	60
1-2	200	55
2-3	200	50
3-4	200	45
4-5	200	40
5-6	200	35
6-7	200	30
7-8	200	20
8-9	200	12
9-10	200	5

Table 5.6 Dimensions of Vertical Cutouts

Station	B (mm)	A (mm)
1	25	44
2	22.5	40
3	20	35

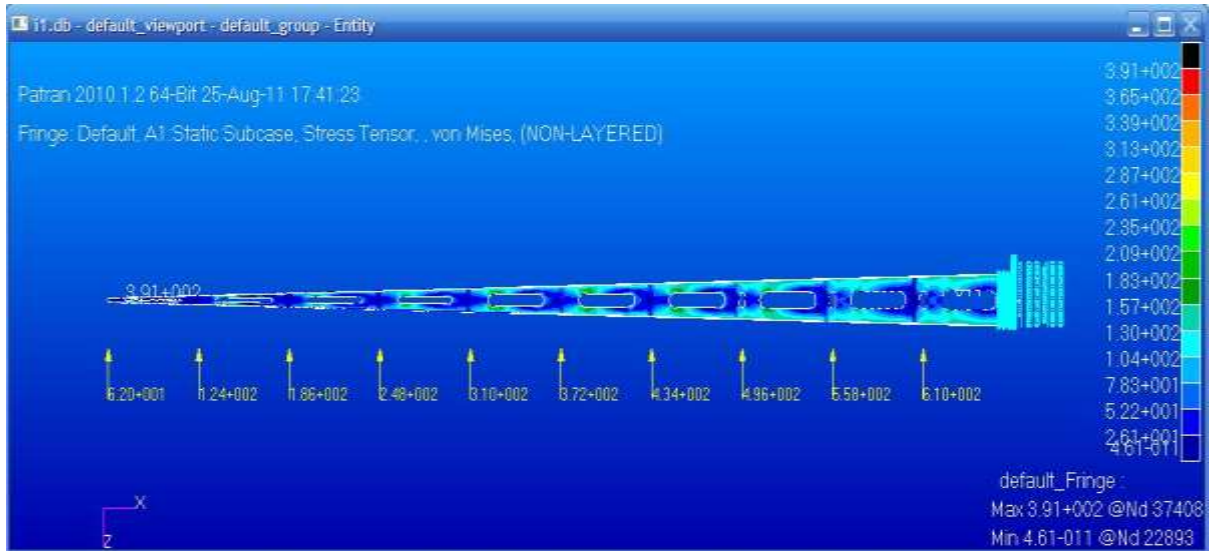


Fig. 5.41 Stress Distribution Contour of Tapered Spar Beam with 10 Horizontal Cut-outs & 3 Vertical Cutouts

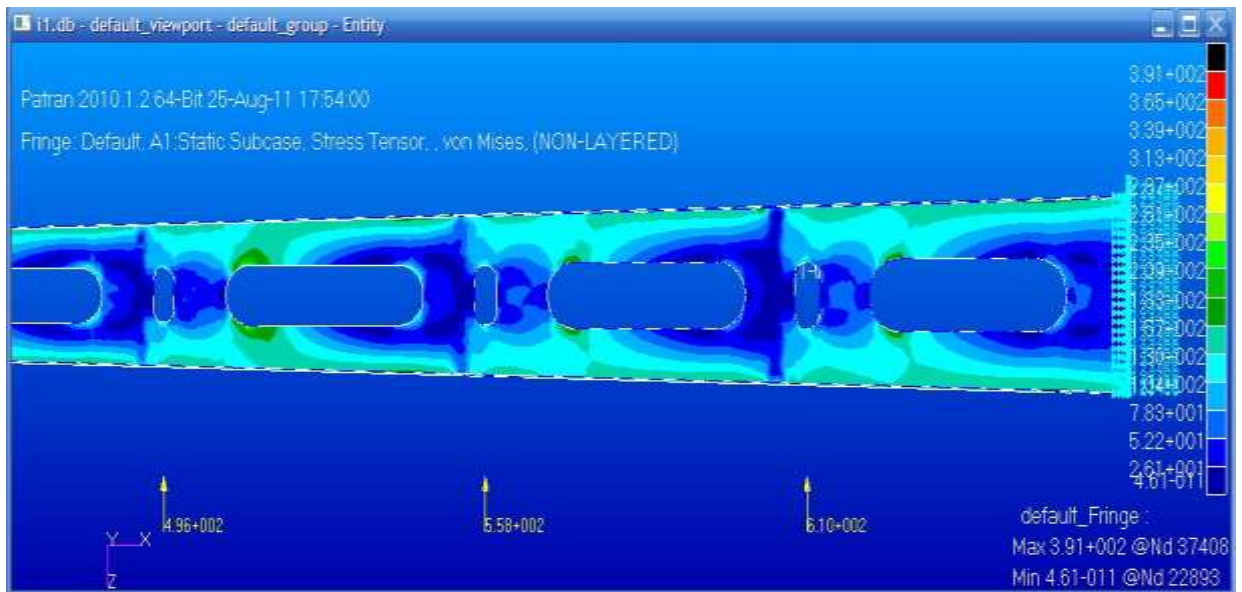


Fig. 5.42 Maximum Stress Region

After applying loads (as shown in Fig) and boundary condition, maximum stress value is now reduced to 391 MPa which is again much greater than the yield strength of the material. Hence this case is also not valid for design of spar beam.

Hence, we will again have to reduce the number of cutouts in the next iteration.

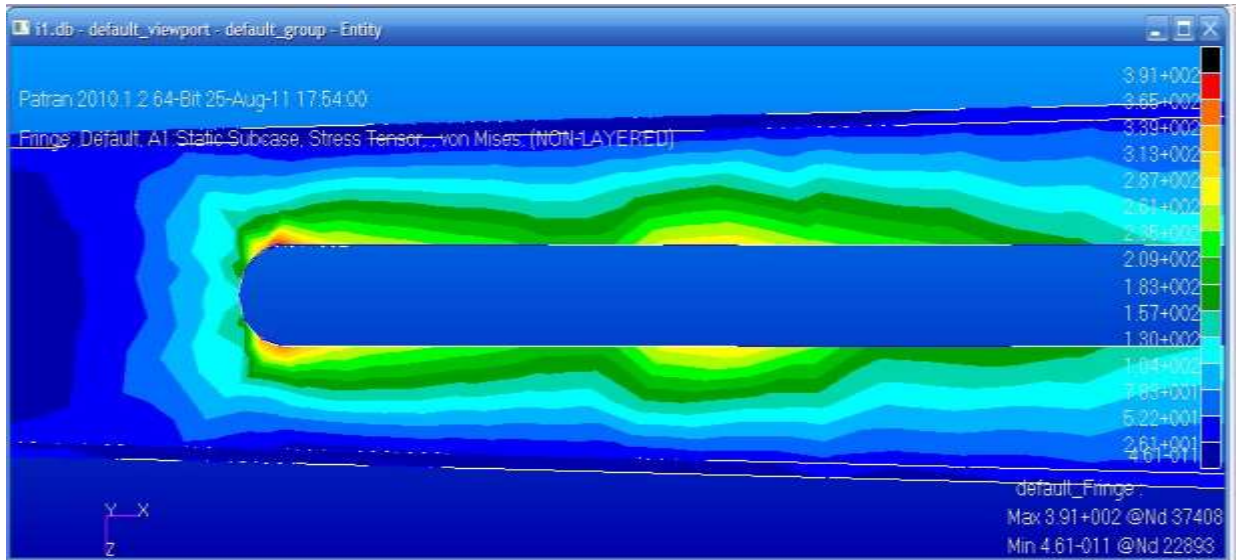


Fig. 5.43 Detailed View

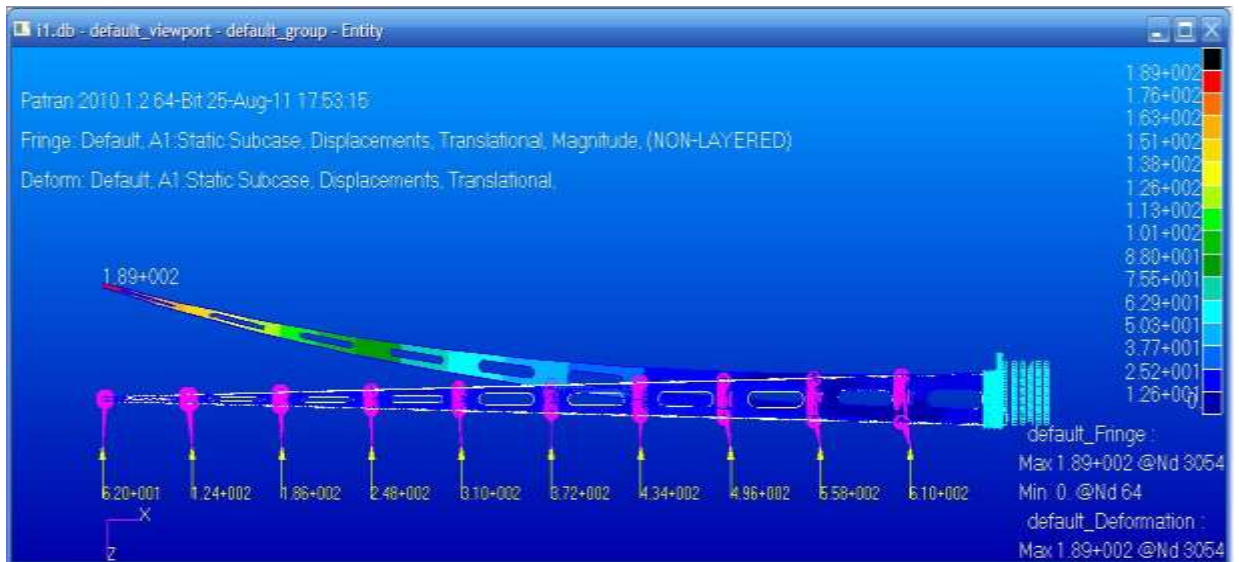


Fig. 5.44 Displacement Results for Tapered Spar Beam with 10 Horizontal Cut-outs & 3 Vertical Cutouts

- **Iteration 7:**

In this iteration, we will introduce horizontal cutouts in first 9 sections and only 3 vertical cutouts at first 3 stations starting from the fixed end.

Table 5.7 Dimensions of Horizontal Cut-outs

Section	B (mm)	A (mm)
0-1	200	60
1-2	200	55
2-3	200	50
3-4	200	45
4-5	200	40
5-6	200	25
6-7	200	10
7-8	200	8
8-9	200	8

Table 5.8 Dimensions of Vertical Cutouts

Station	B (mm)	A (mm)
1	25	55
2	22.5	49.5
3	20	45

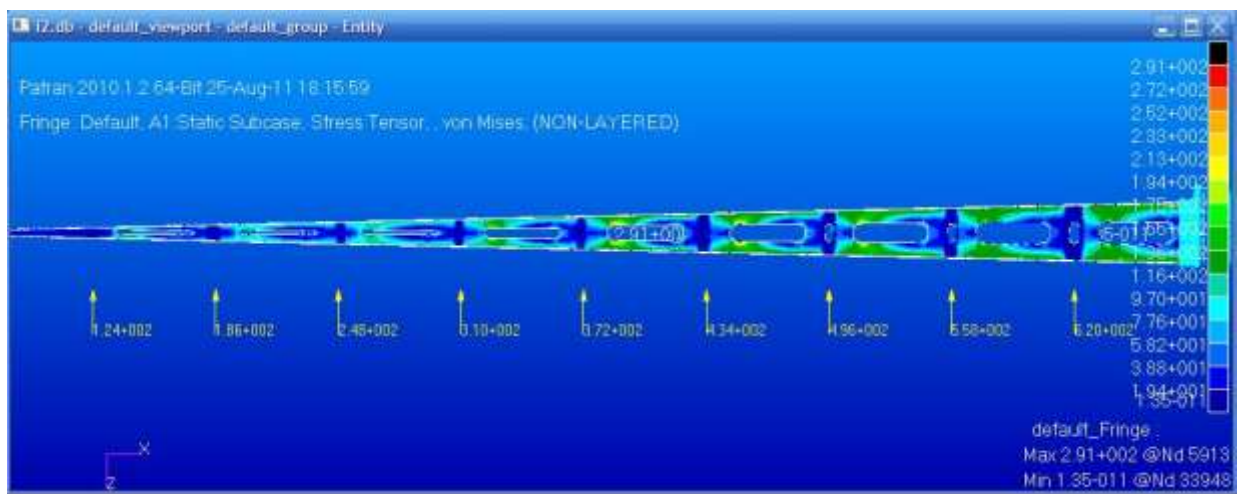


Fig. 5.45 Stress Distribution Contour of Tapered Spar Beam with 9 Horizontal Cut-outs & 3 Vertical Cutouts

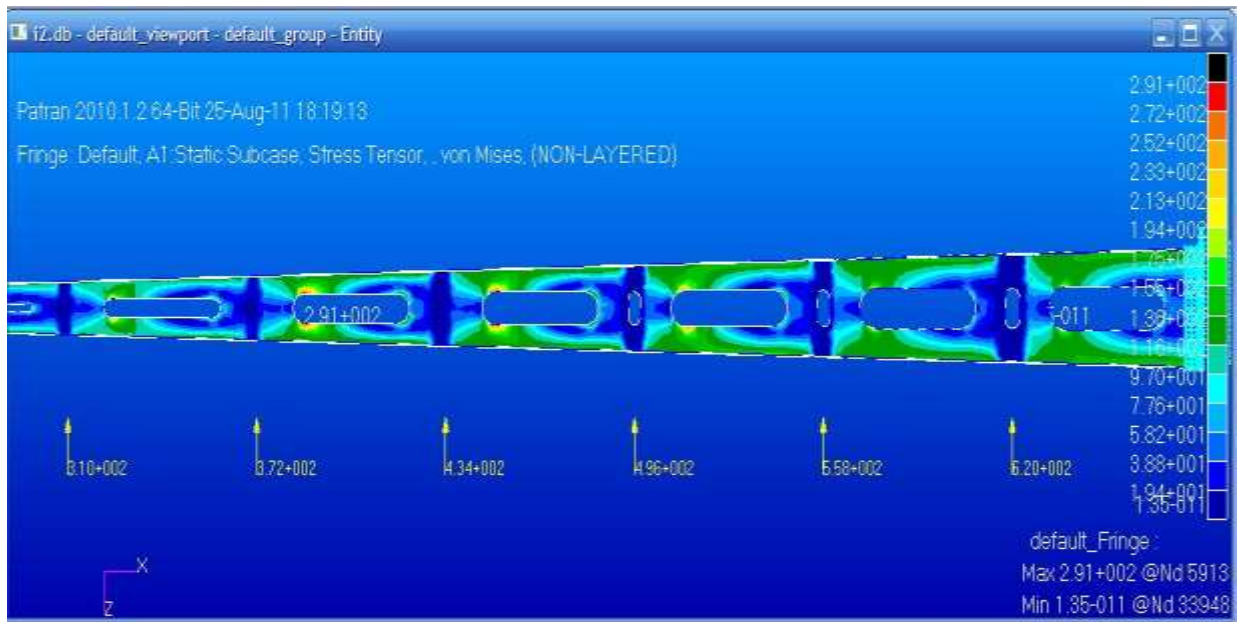


Fig. 5.46 Maximum Stress Region

After applying loads (as shown in Fig) and boundary condition, maximum stress value is reduced to 291 MPa which is little less than the yield strength of the material. Hence this case is perfectly valid for design of spar beam.

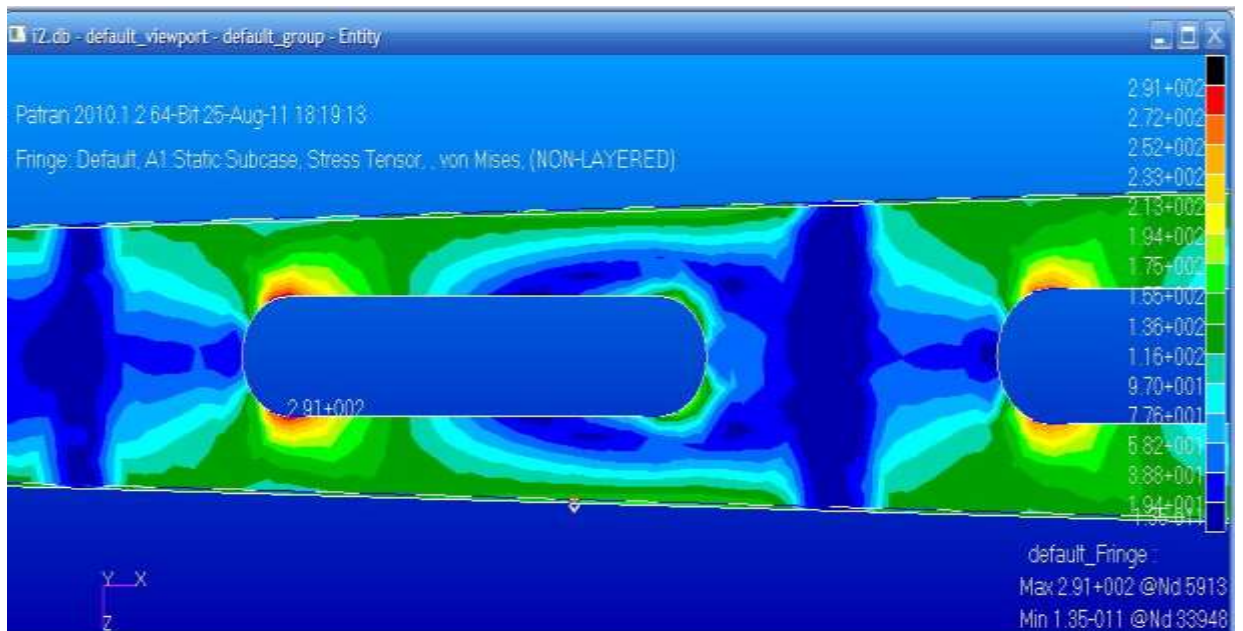


Fig. 5.47 Detailed View

Design and Analysis of A Spar Beam for Vertical Tail of a Transport Aircraft.

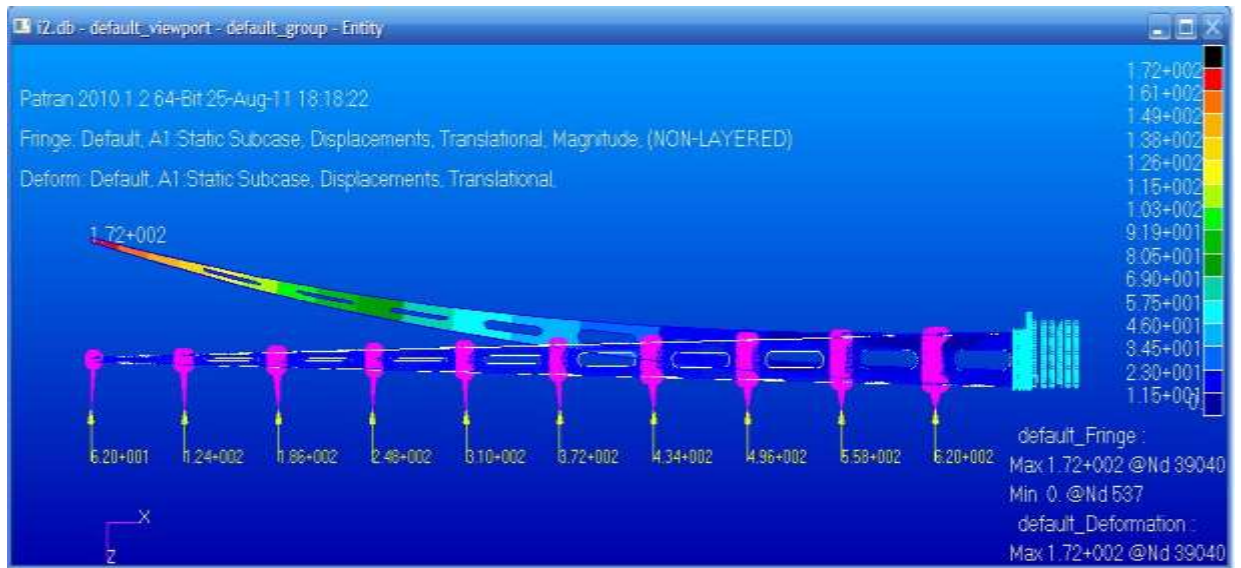


Fig. 5.48 Displacement Results for Tapered Spar Beam with 9 Horizontal Cut-outs & 3 Vertical Cutouts

Mass of Tapered cross-section beam with 9 Horizontal & 3 Vertical Cutouts for $t = 3.5 \text{ mm}$
 $= 2.05 \text{ Kg}$

6. CALCULATIONS

6.1 Calculation of Moment of Inertia at different stations

Table 6.1 Moment of Inertia calculations at different stations

Station No.	D (mm)	B (mm)	T (mm)	D (mm)	$(BD^3-bd^3)/12$ (in mm ⁴)
0	164.106	82.053	8.2053	147.6954	10392469.86
1	149.1	74.55	7.455	134.19	7081601.886
2	134.084	67.042	6.7042	120.6756	4631575.667
3	119.054	59.527	5.9527	107.1486	2878703.263
4	104.003	52.0015	5.20015	93.6027	1676503.257
5	88.921	44.4605	4.44605	80.0289	895856.1646
6	73.789	36.8945	3.68945	66.4101	424802.8611
7	58.566	29.283	2.9283	52.7094	168578.8888
8	43.152	21.576	2.1576	38.8368	49684.92637
9	27.184	13.592	1.3592	24.4656	7824.820437
10	13.592	6.796	0.6796	12.2328	489.0512773

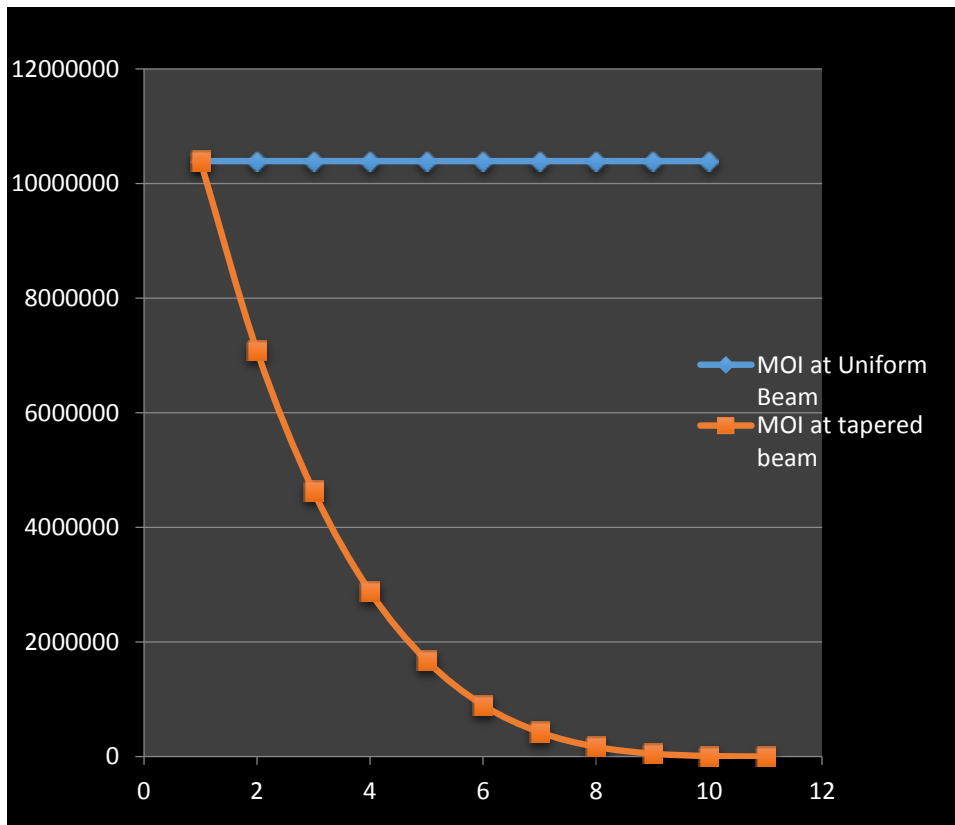


Fig. 6.1 Moment of Inertia at different stations.

6.2 Bending Stress for Uniform I-section Cross Sectional Area

Table 6.2 Bending Stress calculations at different stations for Uniform I-section beam.

Station No.	M (in N-mm)	y (in mm)	I (in mm ⁴)	σ (in N/mm ²)
0	43487700	82.58	10392469.86	345.5592669
1	32615700	82.58	10392469.86	259.1688542
2	23720500	82.58	10392469.86	188.4863672
3	16604400	82.58	10392469.86	131.9408543
4	11069000	82.58	10392469.86	87.95580188
5	6918500	82.58	10392469.86	54.97535597
6	3953400	82.58	10392469.86	31.4142621
7	1976700	82.58	10392469.86	15.70713105
8	790600	82.58	10392469.86	6.282216728
9	197600	82.58	10392469.86	1.570156875
10	0	82.58	10392469.86	0

6.3 Bending Stress for Tapered I-section Cross Sectional Area

Table 6.3 Bending Stress calculations at different stations for Tapered I-section beam.

Station No.	M (in N-mm)	y (in mm)	I (in mm ⁴)	σ (in N/mm ²)
0	43487700	82.053	10392469.86	343.3540146
1	32615700	74.55	7081601.886	343.3545791
2	23720500	67.042	4631575.667	343.3539416
3	16604400	59.527	2878703.263	343.3525544
4	11069000	52.0015	1676503.257	343.3364064
5	6918500	44.4605	895856.1646	343.3586567
6	3953400	36.8945	424802.8611	343.3562475
7	1976700	29.283	168578.8888	343.3627218
8	790600	21.576	49684.92637	343.3231534
9	197600	13.592	7824.820437	343.2384451
10	0	6.796	489.0512773	0

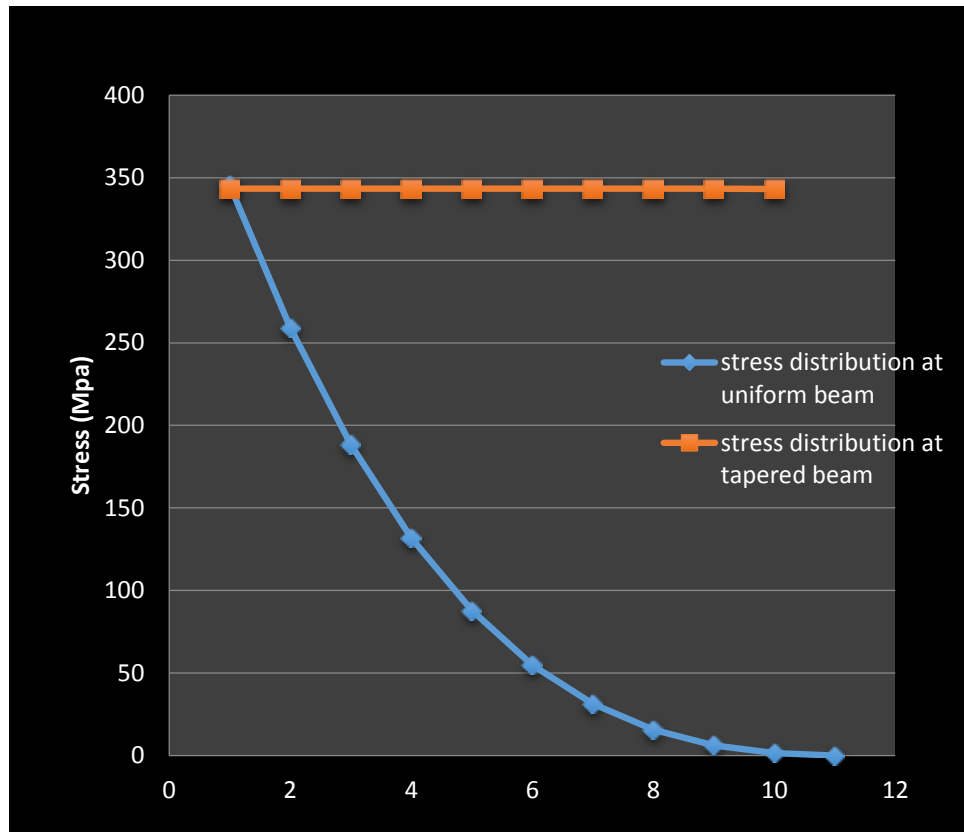


Fig. 6.2 Stresses at different stations

7. RESULTS & CONCLUSIONS

Table 7.1 UTS of beams

Spar Beam Cross-Section	UNIFORM	TAPERED
FEA	43.1 MPa	72.1 MPa

Table 7.2 Experimental value of Aluminium 2024 T-3

Ultimate Tensile Strength	Yield Strength
490 MPa	310 MPa

- **Uniform Cross-section Spar Beam**

The UTS values obtained from FEA are much less than the Experimental UTS & Yield Strength values.

The Stress values show that the Stresses induced are greatest across the station 0-1, i.e., nearest to the fixed end and decreases gradually towards the free end, becoming zero at the free end.

We observe that the further stations carry less stresses. Therefore, we can think of tapering the beam to achieve weight optimization.

- **Tapered Cross-section Spar Beam**

Again, the UTS values so obtained from FEA are still less than the Experimental UTS & Yield Strength values. The stress values so obtained shows that the Stresses are same at all sections throughout the beam.

Thus, there is a scope of reducing the thickness ‘t’ of the spar beam along the span.

As a result, we achieve better strength to weight ratio by decreasing the weight for the same strength.



Table 7.3 Thickness Iteration result

Thickness Iterations	t (mm)	Maximum Stress(MPa)
1	8.205	72.1
2	6.2	106
3	3.5	179

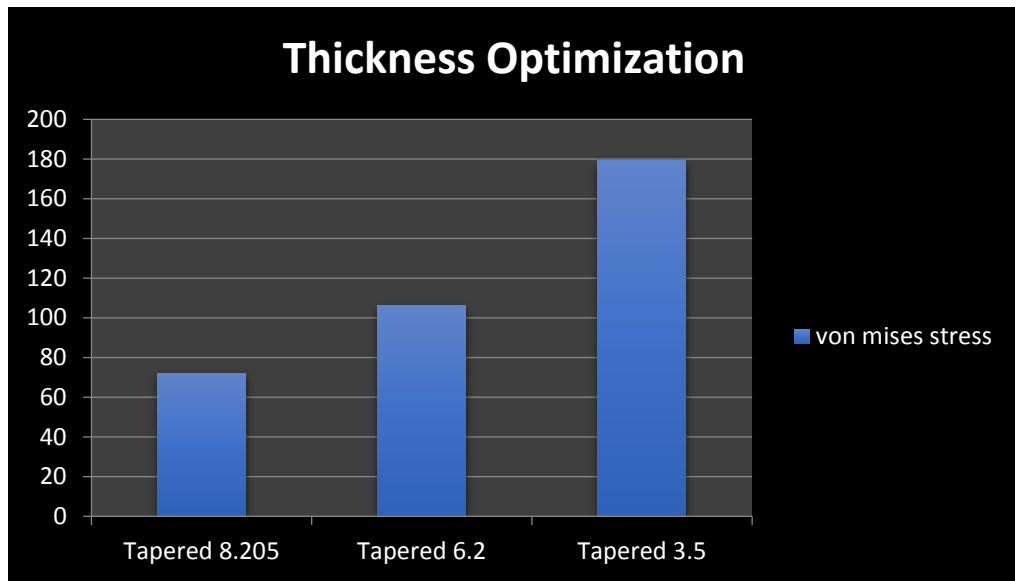


Fig. 7.1 Thickness Iteration result plot

- **Tapered Cross-section Spar Beam With Cut-outs**

Table 7.4 Cutout Iteration results

Cutouts Iterations	Cutout Orientation	t (mm)	Maximum Stress(MPa)
1	Vertical	6.2	126
2	Vertical	3.5	191
3	Horizontal	6.2	200
4	Horizontal	3.5	240

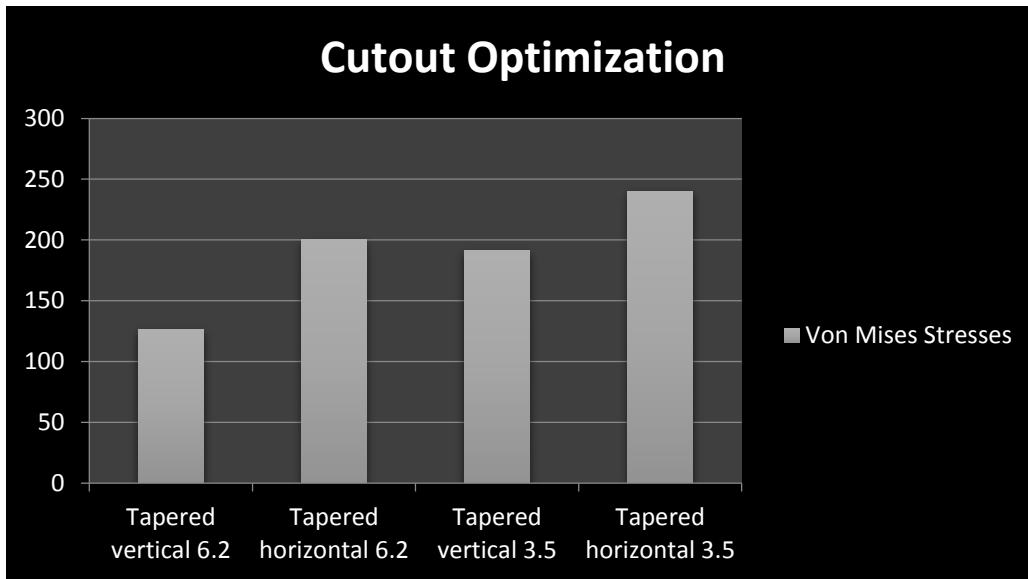


Fig. 7.2 Cutout Iteration results plot

As earlier, the UTS values so obtained from FEA are again less than the Experimental UTS & Yield Strength values.

Thus, several more iterations can be made in the cut-outs. Further iterations will be carried out for the beam with thickness, $t = 3.5$ mm

As a result, we further achieve better strength to weight ratio by decreasing the weight for the same strength.

- **Tapered Cross-section Spar Beam With Mixed Cut-outs for $t = 3.5$ mm**

Table 7.5 Mixed Cutout Iteration results

Cutouts Iterations	Horizontal Cutouts	Vertical Cutouts	Maximum Stress (MPa)
5	10	6	486
6	10	3	391
<u>7</u>	<u>9</u>	<u>3</u>	<u>291</u>

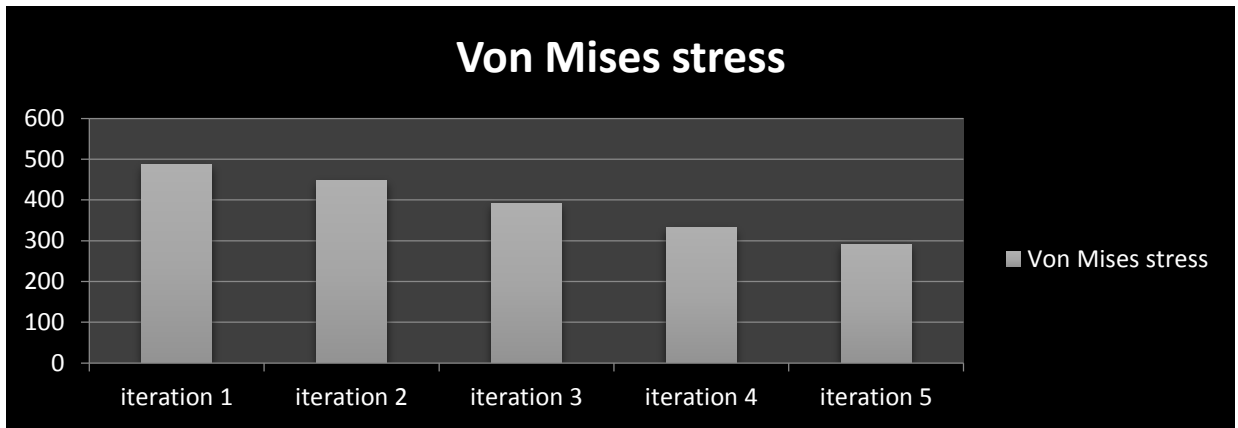


Fig. 7.3 Mixed Cutout Iteration results plot

The maximum stress value for the 7th iteration, i.e., for 9 horizontal cutouts and 3 vertical cutouts is found to be 291 MPa which is little less than the yield strength of the material.

Therefore, the design used in 7th iteration is the final model with best strength to weight ratio.

7.1 Weight optimization of Spar beam

- Mass of Tapered cross-section beam with 6.2 mm thickness = 3.611 Kg
- Mass of Tapered cross-section beam with 3.5 mm thickness = 2.118 Kg
- Mass of Tapered cross-section beam with 9 Horizontal & 3 Vertical Cutouts for t = 3.5 mm = 2.05 Kg
- Weight Optimization:

$$\text{Weight Reduction (\%)} = \frac{(3.611-2.05) \times 100}{3.611}$$

$$= \mathbf{41.34\%}$$

8. REFERENCES

- **Vinod S. Muchchandi, S. C. Pilli (2013) 'Design and Analysis of A Spar Beam For The Vertical Tail of A Transport Aircraft', *International Journal of Innovative Research in Science, Engineering and Technology*, 2(7)**
 - **Immanuel D, Arulselvan K, Maniiarasan P, Senthilkumar S (2014) 'Stress Analysis and Weight Optimization of a Wing Box Structure Subjected To Flight Loads', *The International Journal Of Engineering And Science (IJES)*, 3(1), pp. 33-40**
 - **Vignesh T., Hemnath B.G., Caesar J., Sutharsan P., Chinagounder C. (2014) 'Static Stress and Fatigue Analysis on Vertical Stabilizer of a Typical Trainer Aircraft', *International Journal of Innovative Research in Science, Engineering and Technology*, 3(4)**
 - **Chùn-yun Niu (1988) *Airframe structural design: practical design information and data on aircraft structures*, Hong Kong: Conmilit Press.**
 - **Sun, C. T. (2006) *Mechanics of aircraft structures*, Hoboken, NJ: J. Wiley.**
 - **Thomas Henry Gordon Megson (2013) *Aircraft Structures for Engineering Students*, : Elsevier.**
 - **David J. Peery (2011) *Aircraft structures*, Mineola, N.Y: Dover Publications.**
 - **Daniel P. Raymer (2012) *Aircraft design: a conceptual approach*, Reston, VA: American Institute of Aeronautics and Astronautics.**
 - **Michael Niu, 2011. *Airframe Stress Analysis & Sizing*. Edition. Adaso/Adastra Engineering Center.**
 - **Sridhar Chintapalli (2006) *Preliminary Structural Design Optimization of an Aircraft Wing-Box*, Concordia University, Montreal, Canada.**
-